AN ANALYSIS OF A LIQUID DESICCANT DEHUMIDIFIER REGENERATED WITH WASTE OR SOLAR POWER

Robert George Vorthman

AN ANALYSIS OF A LIQUID DESICCANT DEHUMIDIFIER REGENERATED WITH WASTE OR SOLAR POWER

by

ROBERT GEORGE VORTHMAN, JR.

B.S.E.E., Tri-State College
Angola, Indiana
(1971)

SUBMITTED IN PARTIAL FULFILLMENT
OF THE REQUIREMENTS FOR THE
DEGREES OF

OCEAN ENGINEER

AND

MASTER OF SCIENCE
IN MECHANICAL ENGINEERING

at the

MASSACHUSETTS INSTITUTE OF TECHNOLOGY

May 1977

AN ANALYSIS OF A LIQUID DESICCANT DEHUMIDIFIER REGENERATED WITH WASTE OR SOLAR POWER

by

ROBERT GEORGE VORTHMAN, JR.

Submitted to the Department of Ocean Engineering on May 12, 1977 in partial fulfillment of the requirements for the degrees of Ocean Engineer and Master of Science in Mechanical Engineering.

ABSTRACT

The finned tube contactor of a liquid desiccant (triethylene glycol) dehumidifier system is modeled with a fifth order differential equation to simulate the simultaneous heat and mass transfer associated with conditioning the air. Potential energy saving aspects of the system are discussed. Computer simulation results presented on psychrometric charts show that significant performance is possible with contactors of one half the recommended size. The cycle may be regenerated at 120 to 140°F depending on the system design requirements.

Figure 4 may be used to estimate system performance.

Thesis Supervisor: James D. Felske
Title: Assistant Professor of Mechanical Engineering

ACKNOWLEDGEMENTS

A sincere thank you is made to Professor James D. Pelske for his understanding and guidance.

The patience of my wife, Kathleen, in enduring my endless monologues on desiccants, psychrometry, and computer modeling is appreciated.

Special acknowledgement is due to Ralph Collins, artist extraordinaire.

I am also indebted to the United States Coast Guard for the opportunity to study at M.I.T.

TABLE OF CONTENTS

LIST OF FIGURES AND TABLE

NOMENCLATURE AND UNITS

Abbreviations

LDD	Liquid Desiccant Dehumidification
TEG	Triethylene Glycol

English Letter Symbols

a_C	Cooling area per unit volume for heat transfer, ft^2/ft^3
a_H	Interfacial area per volume for heat transfer, ft^2/ft^3
a_M	Interfacial area per volume for mass transfer, ft^2/ft^3
c,C	Heat capacity at constant pressure, BTU/lb
C_S	Humid heat, BTU (of water vapor-gas mixture)/(lb dry gas)(°F) defined by Eq. (A.22)
C_{SL}	Humid heat, BTU (of TEG-water solution)/(lb TEG)(°F) defined by Eq. (A.33)
D_r	Root diameter of tube, ft
D_v	Diffusion coefficient for water vapor in air, ft^2/hr
F_G	Mass Transfer coefficient, lb water/(hr) (ft^2) defined by Eq. (C.1)
g	Acceleration due to gravity, ft/hr^2
G	Superficial gas (dry air plus water vapor) mass velocity, lb/(hr)(ft^2)

G_{max}	Gas mass velocity at minimum cross section, lb/(hr)(ft^2)
G_s	Superficial solvent (dry air) mass velocity, lb/(hr)(ft^2)
h_G	Contact coefficient of heat transfer between gas and liquid, BTU/(hr)(ft^2)(°F) defined by Eq. (C.2)
h'_G	Contact coefficient of heat transfer between gas and liquid corrected for simultaneous mass transfer BTU/(hr)(ft^2)(°F) defined by Eq. (A.15) and (A.16)
h_l	Contact coefficient of heat transfer between liquid and cooling fin, BTU/(hr)(ft^2)(°F) defined by Eq. (C.13)
h_L	Conduction coefficient of heat transfer in liquid, BTU/(hr)(ft^2)(°F) defined by Eq. (C.11)
H	Enthalpy, BTU/lb
H_D	Heat of dilution (mixing), BTU/lb
k	Thermal conductivity, BTU/(hr)(ft)(°F)
l	Effective fin length, in.
L	Superficial liquid (TEG plus water) mass velocity, lb/(hr)(ft^2)
L_S	Superficial solvent (TEG) mass velocity, lb/(hr)(ft^2)

N_A	Mass transfer flux of water vapor, lb/(hr)(ft^2) defined by Eq. (A.14)
p *	Partial pressure in equilibrium with a liquid solution, mm Hg
p_t	Total pressure, mm Hg
P	Fin pitch, fins/in; Chapter II: pressure
Q_C	Heat removed by cooling coil, BTU/hr defined by Eq. (A.28)
Q_D	Exothermic heat of dilution, BTU/hr defined by Eq. (A.30)
q_s	Heat transfer flux for sensible heat, BTU/(hr)(ft^2)
R	Chapter II: universal gas constant; Appendix B: bond graph resistance
s	Spacing between fins, in.
S	Interfacial surface, ft^2/ft^2 cross section
t	Thickness of aluminum cooling fin, in; temperature, °F
T	Chapter II, temperature, °F
T_{sh}	Horizontal tube spacing, in.
T_{sv}	Vertical tube spacing, in.
U	Over-all coefficient of heat transfer between the liquid and cooling water, BTU/(hr)(ft^2)(°F)
V_f	Water velocity through tube, ft/sec

x	Mass fraction concentration in the bulk liquid, lb water/(lb water + lb TEG)
X	Mass ratio concentration in the bulk liquid, lb water/lb TEG
y	Mass fraction concentration in the bulk gas, lb water vapor/(lb water vapor + lb dry air)
y*	Mole fraction concentration in the gas in equilibrium with the bulk liquid, moles water vapor/(moles water vapor + moles dry air)
y_m	Mole fraction concentration in the bulk gas, moles water vapor/(moles water vapor + moles dry air)
Y	Mass ratio concentration in the bulk gas, lb water vapor/(lb dry air)
Z	Height of finned tube contactor (parallel to flow direction), ft.

Greek Letter Symbols

Γ	Liquid loading per unit width of fin, lb/(hr)(ft)
δ	TEG solution thickness, ft.
η	Fin efficiency, dimensionless
λ	Latent heat of vaporization, BTU/lb
μ	Viscosity at bulk temperature, lb/(hr)(ft)
ρ	Density, lb/ft^3
σ	Ratio of free flow area to face area, dimensionless

ν	Chapter II: specific volume, ft^3/lb

Dimensionless Groups

Pr	Prandtl number ($\mu c_p/k$)
Sc	Schmidt number ($\mu/\rho D_v$)

Subscripts

A	Substance A, water vapor
AL	Substance A, liquid water
B	Substance B, dry air
C	Substance C, TEG
D	Substance D, water plus TEG solution; dilution
f	Cooling water
g,G	Gas
i	Interface
l,L	Liquid
o	At the reference temperature

Bond Graph Symbols

C	Capacitance
C_m	Mass capacitance
C_t	Thermal capacitance
N_A	Mass transfer flux
Q	Heat flux
R	Resistance
R_d	Diffusion resistance
R_i	Interfacial resistance to mass transfer

R_r	Reaction resistance
S_{fd}	Heat of dilution flow source
S_{fl}	Latent heat flow source
t	Temperature
T	Transformer
0	Parallel junction, flows sum to zero
1	Series junction, efforts sum to zero
———	Power bond
——→	Signal bond

I. INTRODUCTION

Definitions

Liquid desiccant dehumidification is the reduction of the water vapor content of a given volume of air by a liquid sorbent which has the property of extracting and holding water vapor brought into contact with it. The terms sorbent and desiccant refer to materials with a large capacity for moisture compared to their volume and weight. The amount of water held by a desiccant will increase or decrease depending on whether the vapor pressure of water above the desiccant is less than or greater than the partial pressure of water vapor in the air in contact with it.

Applications

Dehumidification, whether by liquid desiccants or by other means, has important commercial applications. These include preserving ships and other surplus equipment which would otherwise deteriorate, and preventing condensation damage to cargo and internal structures of ships' holds which transport dry cargo.

Liquid desiccant dehumidification (LDD) was investigated in the 1950's and found to be operational [7],[22]. Currently LDD equipment designed for low pressure steam regeneration is commercially available and is used in the drying of natural gas prior to pipeline transportation. Both hospitals and the food processing industry use LDD not only for temperature and humidity control but also for the bactericidal properties of the family of glycol desiccants. Accepted high equipment cost prevents wider application of LDD for the general purpose of space de-

humidification or space cooling. These costs are on the order of $10 per square foot of contactor in typical LDD systems which remove about 500 pounds of water per hour with dehumidification and regeneration contactor areas of 5000 sq. ft. each [27].

Potential Savings

If the potential to regenerate an LDD cycle at low temperatures is exploited and waste heat or solar energy is utilized, then potential energy savings can be applied against acquisition cost. Such cost may be minimized by rational rather than empirical equipment selection.

A review of current space dehumidification and cooling practice will indicate the potential energy savings of LDD.

In conventional air conditioning systems the air is cooled significantly below the desired temperature to effect moisture removal. (Refer to Figure 1).

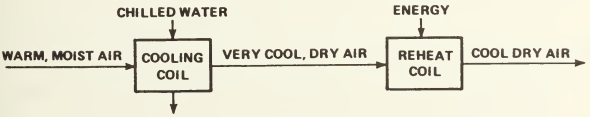

Figure 1. Conventional Air Conditioner with Reheat

Additional energy is used as this very cool, dry air is then reheated to the desired space temperature. The popularity of this system stems from the previously low cost of energy and the simple control system required. One dependent variable, outlet humidity ratio, is uniquely controlled by the chilled water temperature through the condensation of excess moisture above the dew point temperature. The other dependent variable, desired space temperature, is now uniquely controlled at a constant humidity by the quantity of reheat energy added.

The control system complexity increases when an attempt is made to save reheat energy by mixing the very cool dry air with warm moist air bypassed around the cooling coil. (Refer to Figure 2.)

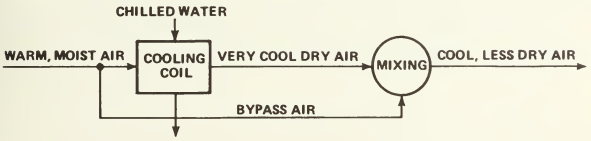

Figure 2. Conventional Air Conditioner with Bypass Mixing

Both of the two independent variables, chilled water temperature and bypass air flow rate, simultaneously modify both of the dependent variables, outlet air temperature and humidity ratio.

The LDD system can save the energy of excess chilling for moisture removal through its ability to dehumidify at ambient temperatures. Removal of the latent heat of condensation is the primary function of the cooling water. (Refer to Figure 3.)

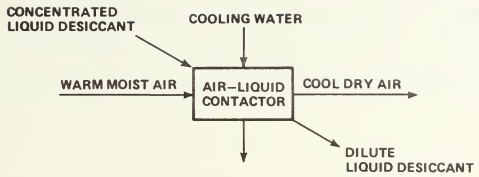

Figure 3. Liquid Desiccant Dehumidification System

The dehumidification contactor of the LDD system, a three fluid heat exchanger in which mass transfer between two of the fluids occurs, can supply cool, dry air without further heating or cooling. Thus, the reheat energy can also be saved.

In the LDD contactor the two dependent variables, air temperature and humidity ratio, are controlled by the independent variables, liquid desiccant concentration and cooling water temperature. A tradeoff for the potential energy savings of excess chilling and unnecessary reheat is a control system of sophistication similar to that of the bypass system shown in Figure 2.

The LDD cycle compares favorably to an alternative technique for space cooling such as the lithium bromide absorption cycle. While the absorption cycle is closed and the desiccant cycle is open, both systems have coefficients of performance on the order of 0.6 [11]. The absorption cycle requires regeneration temperatures around 200°F, while the

LDD cycle can be regenerated at temperatures around 140°F. Of these two systems the absorption system has been the subject of considerable analysis and simulations [9]; however, there is no well-established technique for space cooling or dehumidification with low temperature regeneration.

Purpose

In view of the above, a model for analysis of the liquid desiccant dehumidifier contactor of Figure 3 is presented as the basis for a rational design. The primary function of the model is to assure that the contactors are not over-specified so that acquisition costs may be kept as low as possible. The contactors (dehumidification and regeneration) represent a significant portion of the total cost of an LDD system.

Empirical equipment selection of the contactors is standard practice and can result in overspecification to ensure proper operation. Manufacturers' application recommendations specify equipment which operates with the exit conditions of air and liquid temperatures, humidity ratio, and desiccant concentration at equilibrium.

By contrast, rational design implies more than black box modeling of the contractor. The computer model of the contactor which was developed is based on a complete set of energy balances, material balances, rate equations, and equilibrium relationships. Through computer simulation of the heat and mass transfer in the contactor, the rate at which the temperatures, humidity ratio, and desiccant concentration approach equilibrium as a function of flow distance can be studied. With a specific design the contactor flow length and associated cost can be compared

to the incremental heat and mass transfer of additional contactor flow length increments.

II. PSYCHROMETRY

The Psychrometric Chart

Here psychrometry is concerned with the determination of the properties of the mixture of air and water vapor as the mixture flows through the contactor. These properties are conveniently diagrammed in an abbreviated psychrometric chart, Figure 4, which plots dry bulb temperature, humidity ratio, wet bulb temperature, saturation temperature, and relative humidity for the air-water vapor mixture.

Dry bulb temperature represents the air and liquid contact temperature and is the abscissa.

Humidity ratio (H.R.) is the pounds of water carried by one pound of dry air. Alternatively, grains per pound of dry air (grains) is used where 7000 grains equal one pound of water. The ordinate shows both humidity ratio and grains.

Relative humidity is the ratio of partial pressure of the water vapor to the vapor pressure of water at the air temperature and is indicated by the dotted lines. Relative humidity is expressed in percent.

Wet bulb temperature lines run upward and to the left to the saturation curve and very nearly represent the path followed by adiabatic (spray) cooling.

Dew point temperature is the temperature to which the mixture must be cooled to become saturated and is found by following a horizontal line to the saturation temperature curve.

Saturation temperature represents the maximum moisture the air can

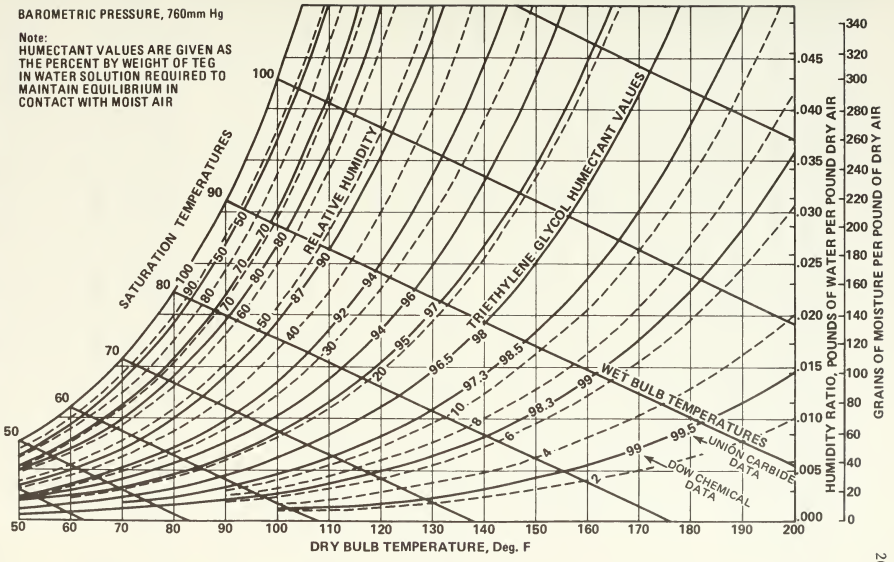

Figure 4. Triethylene Glycol Equilibrium Humectant Values on Psychrometric Chart

hold before fogging ensues.

Enthalpy and specific volumes are plotted on more detailed charts [26]. Any two of these parameters specify the air-water vapor mixture and allow all the others to be determined. The remaining parameter, humectant value, is discussed later under its own section.

Dry bulb temperature and humidity ratio were chosen as the two dependent variables of interest because: (1) dry bulb temperature is easily measured and has significance to people; and (2) the humidity ratio directly represents the water content of the air and is based on one pound of dry air which is a constant in any psychrometric process.

Psychrometric Chart Processes

The process of heating or cooling moist air above the dew point is represented by a horizontal line since the humidity ratio is unchanged. This process is known as sensible heating or cooling.

The process of cooling below the dew point entails condensation of vapor and is represented by a horizontal line extending left to the saturation curve where the process follows the curve to a lower humidity ratio. This is roughly the dehumidification process of conventional air conditioning.

A downward vertical line on the chart represents an isothermal dehumidification process or latent cooling. This may be accomplished directly by the LDD system with cooling to remove only the latent heat of condensation.

Liquid Desiccants

A liquid desiccant removes water vapor from the air at a rate direc-

tly proportional to the difference between the partial pressure of the water vapor immediately above the liquid desiccant. The partial pressure of water vapor in the air is reduced and the liquid desiccant is diluted in the process until equilibrium occurs. The process may be reversed by heating the desiccant. That is, the liquid desiccant is concentrated as the partial pressure of water vapor in the air increases. The vapor pressure of the liquid desiccant is a function of temperature and concentration.

Humectant Values

Equilibrium humectant values are the percent by weight of a liquid desiccant in water solution required to maintain vapor pressure equilibrium in contact with air of various temperatures and humidity ratios. The humectant values for triethylene glycol (TEG) were added to the standard psychrometric chart to produce a convenient diagram revealing the relationship between TEG concentration and the air-water vapor mixture at equilibrium. The humectant values on Figure 4 were developed from graphs of the vapor pressure of water over triethylene glycol of various weight concentrations and temperatures [28] [37]. These equilibrium humectant values give an indication of the TEG concentration necessary to dehumidify to a specified outlet condition with a constant TEG concentration.

The solid lines which are the TEG equilibrium humectant values represent slightly different TEG weight concentrations in the 90% to 99% range depending on the data base: Union Carbide [37] or Dow Chemical [28]. A third source [12], presented data for only three concentrations, 40%,

60%, and 80% and these were consistent with the first two sources within 5%. The vapor pressures presented by Union Carbide and Dow Chemical differ by approximately 20% at 90% concentration and 100% at 98% concentration. Union Carbide data presented the higher vapor pressures. The more conservative humectant values during dehumidification are derived from the Union Carbide data while the more conservative humectant values during regeneration are derived from the Dow Chemical data.

In the area of Figure 4 in which dehumidification takes place, 70 to 80 °F and 0.010 H.R., the change in TEG humectant value with respect to temperature is about 1%/°F. At a 0.025 H.R. and 120 to 130 °F where regeneration can take place, the ratio is about 0.2%/°F which indicates that TEG regeneration should not be particularly sensitive to regeneration temperatures.

Vapor Pressure Prediction

An equation for the equilibrium partial pressure above the liquid desiccant is necessary for the computer simulation. In addition to accuracy, a suitable equation will have continuous derivatives over its range and will be relatively efficient with respect to calculation time. Two relationships with these characteristics which predict vapor pressure as a function of TEG contact temperature and TEG weight concentration were developed with the aid of a curve fitting program and a programmable calculator:

From Dow Chemical data,

$$p^* \text{ [mm Hg]} = \exp\left[\frac{-9346}{T+460} + 20.5749 - \frac{21.36(98-P_T)}{625 + (98-P_T)^2} + \frac{98-P_T}{495} + \frac{\left(1 - \left(\frac{P_T}{99}\right)^{13.5}\right)^{0.6024} - 1}{0.28294}\right] \qquad (2.1)$$

From Union Carbide data,

$$p^* \text{ [mm Hg]} = \exp\left[\frac{-9259}{T + 460} + 20.407 - 1.4333\left(\frac{1}{100.5 - P_T}\right)^{1.5} + \frac{\left(1 - \left(\frac{P_T}{99.5}\right)^3\right)^{0.167} - 1}{0.26921}\right] \quad (2.2)$$

where T = contact temperature, °F

P_T = TEG weight fraction concentration, %.

Both relationships are accurate within about 3% within the ranges $40 \leq T \leq 300$, $75 \leq C \leq 99$ and are slightly less accurate for $0 < C < 75$, Eq. (2.2) was used exclusively in the simulation.

Vapor Pressure Correlation

The method used in synthesizing equations (2.1) and (2.2) is based on the Clausius-Clapeyron equation which relates the slope of the vapor-pressure curve to the latent heat of vaporization

$$\frac{dP}{dT} = \frac{\lambda}{T(v_G - v_L)} \quad (2.3)$$

where v_G = specific volume of the saturated vapor

v_L = specific volume of the saturated liquid

λ = latent heat of vaporization

Using the ideal-gas law and neglecting v_L in comparison with v_G

$$d \ln P = \frac{dP}{P} = \frac{\lambda dT}{RT^2} \quad (2.4)$$

If λ is fairly constant over the temperature range

$$\ln P = -\frac{\lambda}{RT} + \text{constant} \quad (2.5)$$

Equation (2.5) suggests that a plot of log P against $\frac{1}{T}$ will be linear over small temperature ranges. Antoine's equation published in 1888 allows for slight variation of λ with temperature [26]

$$\ln P = a - \frac{b}{T + c} \tag{2.6}$$

and is probably the best vapor-pressure correlation equation for a simple, three-constant (a, b, and c) equation. Equation (2.6) is the basis for equations (2.1) and (2.2).

III. LIQUID DESICCANT DEHUMIDIFICATION SYSTEM

Operating Cycle

One system for liquid desiccant dehumidification (LDD) is shown in Figure 5. The dehumidifier section on the left accepts warm moist air from the atmosphere and contacts the air with the liquid desiccant in the dehumidifier contactor. Intimate contact between the air and desiccant over a large area occurs through the formation of a thin film of desiccant as it is sprayed over the extended surface contactor. The heat of condensation and the heat of dilution flow through the liquid to the cooling water which can be sea water, well water, or water from a cooling tower. The quantity of cooling water required is strongly dependent on the sensible and latent heat removed from the air by the liquid desiccant and weakly dependent on the desiccant circulation rate between the dehumidifier and regenerator.

The air leaves the contactor flowing downward with entrained desiccant and loses most of the liquid to the sump while crossing it. The remainder of the entrained liquid is eliminated as the cool, dry air flows upward to the controlled space.

The dry bulb temperature of this cool, dry air is weakly dependent on the water removed from the air but is strongly dependent on the temperature of the liquid desiccant. Accordingly, the air flowing through the dehumidifier can be warmed or cooled as it is dried depending on the temperature of the liquid desiccant and the temperature of the cooling water.

Concentration of the liquid desiccant is more easily achieved with

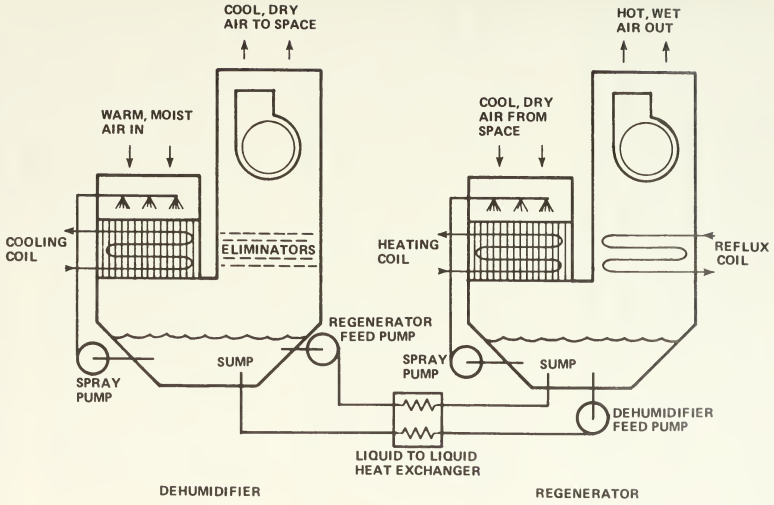

Figure 5. Four Pump Liquid Desiccant Dehumidification System

dry air which would normally be exhausted from the dehumidified space, but can also be achieved with outside air. The heat of vaporization and dilution is supplied through the heating coil in the regenerator contactor to the liquid desiccant as it contacts the relatively dry air. Heating evaporates the liquid desiccant though at a much reduced rate than that of the water. A reflux coil maintained at about 90 °F is used as a condenser for the desiccant to prevent excessive loss in the hot exhaust.

Figure 5 also shows the four pumps necessary for the liquid desiccant movement--two spray pumps and two feed pumps. The liquid-to-liquid heat exchanger between the conditioner sump which is slightly warmer than the cooling water, and the concentrator sump which is slightly cooler than the heating water, improves the system thermal efficiency. An air-to-air heat exchanger between the hot wet exhaust and the cooler inlet air of the regenerator will also increase the system thermal efficiency.

Figure 6 shows a similar system with a combined sump which requires only one pump. While this system is more compact and uses fewer pumps, thermal efficiency can be degraded since the sump operates at a mean temperature. With equal dehumidifier and regenerator desiccant recirculation rates the sump operates as a counter flow heat exchanger with an effectiveness of 0.5, or less than is normally expected from the counter flow heat exchanger of Figure 5.

In either system the solution in the sump will require treatment as it will concentrate solids absorbed from the air.

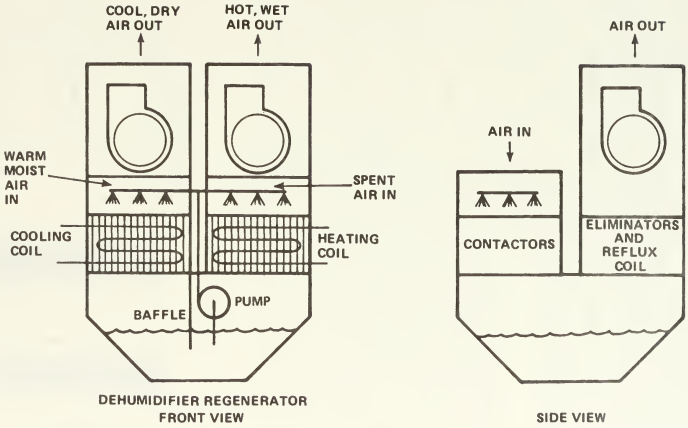

Figure 6. One Pump Liquid Desiccant Dehumidification System

Air-Desiccant Contactor

The contactor is the part of the system in which the air is brought in contact with the liquid desiccant for dehumidification or regeneration. The contactor should have high heat and mass transfer coefficients but yet have relatively low air flow resistance. The contactor should also be light, compact, inexpensive and retain its heat and mass transfer characteristics after extended use.

Although the contactor may consist of a simple spray with the resulting air-desiccant interface being the surface of droplets, entrainment would be excessive since the finely divided liquid is difficult to separate from the air. In addition, it would be difficult to remove the heat of condensation and dilution. A drop spray onto extended surface finned tubes, Figures 7 and 8, prevents atomization of the liquid desiccant and has a better mass transfer capacity per volume than a simple spray [33].

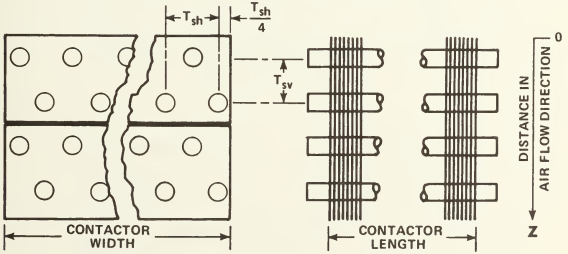

Figure 7. Four Row Finned Tube Contactor Dimensions

Dimensions for Figure 7

T_{sh} = 2.00 in T_{sv} = 1.73 in

Width = 48 in Length = 127 in

Height = 6.69 in/(four rows)

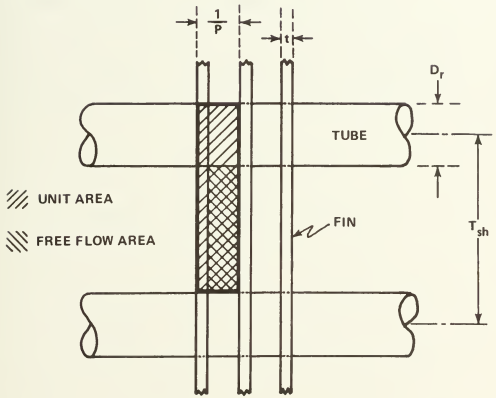

P = 5 fins per inch D_r = 0.75 in

t = 0.010 in T_{sh} = 2.00 in

Figure 8. Dimensions for Determining Free Flow Area of Contactor

The cooling water flows through the tubes in a parallel-counter-flow configuration with an even number of tube passes, while the air and liquid desiccant flow over the extended surface. Thus, the dehumidification contact surface and cooling coil are conveniently packaged in one unit. The cooling water serves to: (1) keep the desiccant cool and thus lower the vapor pressure; and (2) cool the air.

The regenerator contactor has the same physical characteristics and performance criteria as the dehumidifier contactor, although the size may differ because of different air flow and liquid desiccant recirculation rates. Therefore, the computer model presented later simulates the heat and mass transfer of both the dehumidifier and regenerator contactors.

The air flow can be either parallel with or counter to the liquid desiccant flow direction, depending on the particular application. Due to the dilution of the liquid desiccant as it flows through the contactor, the exit humidity ratio is not as low as can be achieved with the counter flow arrangement. However, the downward parallel flow configuration does not inhibit spraying the liquid on the contactor and allows some separation of the liquid and air by a reversal of flow direction.

The parallel flow configuration is best suited for the processing of large volumes of air, while the counter flow configuration can deliver the very dry air needed in manufacturing operations such as the handling of hygroscopic materials. The parallel flow configuration represents our physical system.

Other System Equipment

Other equipment items, such as the main circulating blowers or liquid sorbent pumps, should be selected on the basis of good engineering design with cognizance of the difficulty of containing TEG because of its propensity to leak past defective fittings or packings.

LDD System Advantages

1. Low temperature regeneration as opposed to other thermal cycle air conditioners is possible and allows more efficient operation of solar collectors.

2. Regeneration is not very sensitive to heating water temperature, unlike other thermal cycle air conditioners.

3. Solar or recovered waste power can be used to regenerate the liquid desiccant.

4. The system is simple in construction and operation since the cycle is without high pressure liquids or gases.

5. Precise control of air temperature and humidity results from a specific TEG concentration and cooling water temperature.

6. Co-sorption benefits include the removal of bacteria, odors and various airborne irritants [1].

7. The expense of a separate cooling coil can be saved or a smaller after cooler can be specified if chilled water is used in the dehumidification contactor.

8. Excess dehumidification capacity when obtained from low cost waste heat or solar energy may be advantageously converted to sensible cooling by spray cooling. The spray process cools and humidifies essentially

along the lines of constant wet bulb temperature in Figure 4.

9. In ocean engineering applications dew point temperatures on the order of 10 °F below the structure temperature are required to prevent condensation [10]. The combination of LDD and cold sea water can produce sub-freezing dew point temperatures as the antifreeze qualities of TEG prevent contactor frost accumulation.

IV. METHOD OF ANALYSIS

Mathematical Model

The analysis of the contactor is based on the development of a mathematical model suitable for a computer simulation. The substance of the model developed is presented here; detailed information may be found in the appendices.

The model of the contactor is a fifth order differential equation composed of three first order differential equations for heat transfer and two first order differential equations for mass transfer. The three heat transfer state variables are the gas, liquid, and cooling water temperatures as shown in Figure 9.

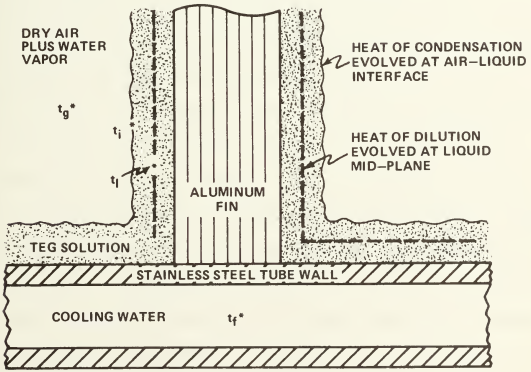

Figure 9. Locations of Representative Temperatures and Sources

TEG Solution thickness	0.007 to 0.010 in
Fin thickness	0.010 in
Tube wall thickness	0.035 in
Tube diameter	0.750 in O.D.

Dimensions for Figure 9.

The two mass transfer state variables are the masses of the gas, (water vapor plus dry air), and liquid, (water plus TEG).

All differentials are taken with respect to flow distance in a steady state model. This is a reasonable assumption, as start up transients will be negligible within a minute or two of operation from a determination of the system RC time constants.

Actual variables used in the program for the mass state variables are the superficial mass velocities of the gas and liquid. Thus, the five independent variables in this model are t_g, t_l, t_f, G, and L. All the other variables are dependent variables and can be calculated from known relationships with knowledge of the five independent variables.

Two distinct methods were used to develop the mathematical model. Appendix A presents a derivation using the traditional method for analyzing mass transfer operations based on material and energy balances in control volumes of a differential section of the contactor. Appendix B uses a general method. It develops a bond graph model of the contactor from which the governing differential equations rigorously follow. The equations developed by the two methods are equivalent.

The five diffenential equations from Appendix A and B are:

$$\frac{dt_g}{dZ} = \frac{t_i - t_g}{R_g C_g} \tag{4.1}$$

$$\frac{dt_l}{dZ} = \frac{t_f - t_l}{R_f C_l} + \frac{t_i - t_l}{R_l C_l} + \frac{Q_D}{C_l} \tag{4.2}$$

$$\frac{dt_f}{dZ} = \frac{t_l - t_f}{R_f C_f} \tag{4.3}$$

$$\frac{dG}{dZ} = - N_A a_M \tag{4.4}$$

$$\frac{dL}{dZ} = N_A a_M \tag{4.5}$$

where t_i, a dependent variable, is

$$t_i = \frac{N_A(1094 + 0.445t_g) + \frac{t_g}{R_g} + \frac{t_l}{R_l}}{N_A + \frac{R_l + R_g}{R_l R_g}} \tag{4.6}$$

Simulation

These five differential equations and the other supporting equations listed in Appendix B which calculate variables such as the mass transfer flux, humidity ratio, and TEG weight fraction concentration form a subroutine. A master program uses the forth order Runge-Kutta method and this subroutine to produce an incremental numerical solution.

Inputs number 19. The geometry of the contactor is specified with eleven inputs. Initial temperatures take three inputs. Flow rates and concentrations each take two inputs and a final input controls the in-

crement size and the stability of the solution.

A substantial portion of the subroutine calculates initial values of approximately 100 variables including the fluid properties and transfer parameters discussed in Appendix C.

A minor portion of the subrountine is repeatedly called during the actual solution. Even so, approximately three minutes are required to calculate the 2500 increments of a 16 row contactor simulation. Each of the five state variables is calculated four times per increment while the auxiliary variables are calculated only once per increment.

The primary outputs of interest are the state variable t_g and the auxiliary variables: Y, humidity ratio; P_T, percent TEG weight fraction concentration; and Z, the distance in air flow direction. Cross plots of t_g and Y produce operating lines on psychrometric charts while cross plots of P_T and Z show the regeneration of the TEG.

V. RESULTS OF SIMULATION

Dehumidifier Contactor

In assessing the performance of the dehumidifier contactor, the operating line on a psychrometric chart furnishes the pertinent information: the inlet and exit conditions and the path between them. The psychrometric chart, Figure 10a, displays a parametric study of dehumidifier operating lines for three TEG inlet concentrations, 92%, 94% and 96% and for three cooling water temperatures, 60°, 70° and 80°F. All simulations begin at 92 °F dry bulb and 76 °F wet bulb (approximately 50% relative humidity) which is a typical outdoor summer temperature specification for performance rating of air conditioning units.

Marks placed on the operating lines of Figure 10a represent equal flow distances of four rows (6.69 inches) except for the special mark which represents conditions two rows (3.34 inches) from the inlet (top of figure). The parameters specified in the figure are the manufacturer's recommendations for a 16 row contactor. For all nine simulations the mark indicating 8 rows is very close to the 16 row mark (within 2 to 4°F and 3 to 4 grains), and represents a 50% savings in contactor acquisition cost. Also, a 4 row contactor using 60°F cooling water is nearly equivalent in performance to a 12 row contactor using 70°F cooling water for the same TEG inlet concentration. Such equivalent performance points can be the basis for optimizing cooling water operating costs and equipment acquisition costs for a specific application.

The dilution vs. flow distance of the TEG solution for the simula-

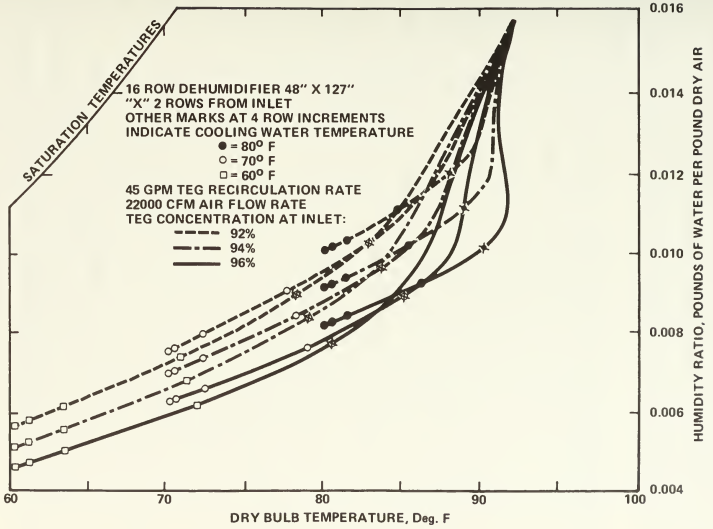

Figure 10a. Dehumidifier Operating Lines for Three TEG Concentrations and Three Cooling Water Temperatures on Psychrometric Chart

tions of Figure 10a is presented in Figure 10b. In Figure 10b, for the same inlet TEG concentrations, the lowest exit concentrations correpsond to the lowest temperature cooling water simulations and the drier conditioned air. The data on Figures 10a and 10b are from the same simulations.

A correlation of Figures 10a and 10b with the equilibrium humectant values of Figure 4 shows that the exit conditions of the 16 row contactor, operating as recommended by the manufacturer, are at equilibrium. For example, from Figure 10b an exit TEG solution concentration of 90% corresponds to an inlet concentration of 94% with 60°F cooling water. On Figure 10a the 94% simulation with 60°F cooling water has exit conditions of 60.5°F and 0.005 H.R. or 35 grains. On Figure 4 a dry bulb temperature of 60.5°F and a 0.005 H.R. corresponds to a TEG equilibrium humectant value of 90% (the Union Carbide data base is used in the computer simulation), which is the exit TEG concentration of Figure 10b.

When psychrometric processes are graphically displayed in the literature the path lines are often straight. The path lines for the liquid desiccant dehumidification simulation are not straight and can be divided into two regions (Refer to Figure 10a.) The first region is nearly all latent cooling (isothermal dehumidification) in which the ability of the cooling water to perform sensible cooling (dry bulb temperature change) is inundated by the exothermic condensation process. In the second region sensible cooling is more pronounced.

The first region physically represents the flow through approximately the first two rows of a 16 row finned tube contactor or approxi-

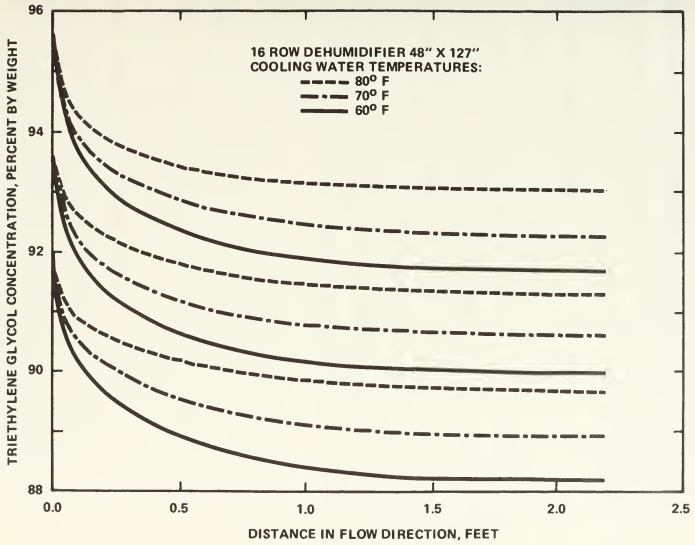

Figure 10b. Dehumidifier TEG Concentration vs. Flow Distance

mately 3.34 inches through a contactor 26.75 inches high. The combination of a high rate of mass transfer at the inlet (see Figure 11) and the associated heat of condensation partially explain the nearly isothermal region. The exothermic heating due to mass transfer is obvious in Figure 12 which shows the variation of the liquid, interface, and air temperatures against distance.

Chemical engineers frequently use a graph of the operating line and equilibrium curve in analyzing the absorption of a substance in gas-liquid operations. Figure 13 shows these lines for the present system. Some simplifications of the calculation procedure can be made if the two lines are straight or are straight and parallel [23]. However, for the LDD system these lines are not straight because of the temperature influence on the equilibrium vapor pressure and hence a computer simulation is required.

The operating line of Figure 13 represents the local mole fraction of water vapor in the air at the local mole fraction of water in the TEG solution. The equilibrium curve represents the equilibrium mole fraction water vapor in air at the local mole fraction water in the TEG solution.

The simulations for Figure 10a were iterated to achieve identical inlet and exit TEG solution temperatures. This corresponds to recirculating the solution through the contactor. Thus, the sump temperature for each simulation is slightly less than the air outlet temperature. The greatest change in liquid temperature is near the inlet (refer to Figure 12) so that the liquid temperature at the 8 row point of a 16 row contactor differs little from the liquid temperature at the exit. For

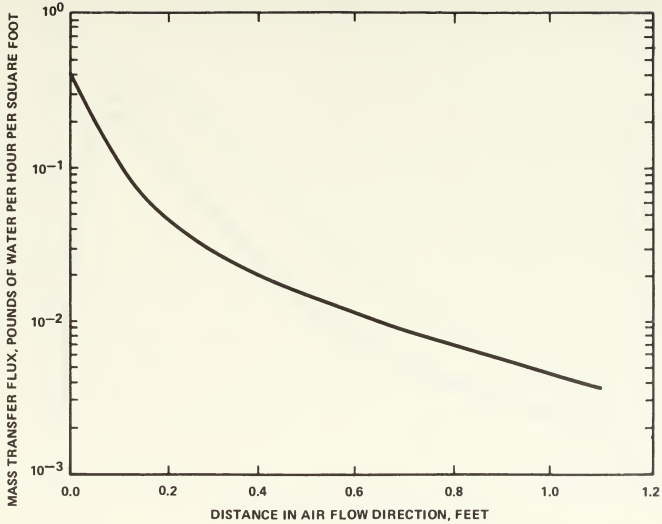

Figure 11. Mass Transfer Flux vs. Flow Distance

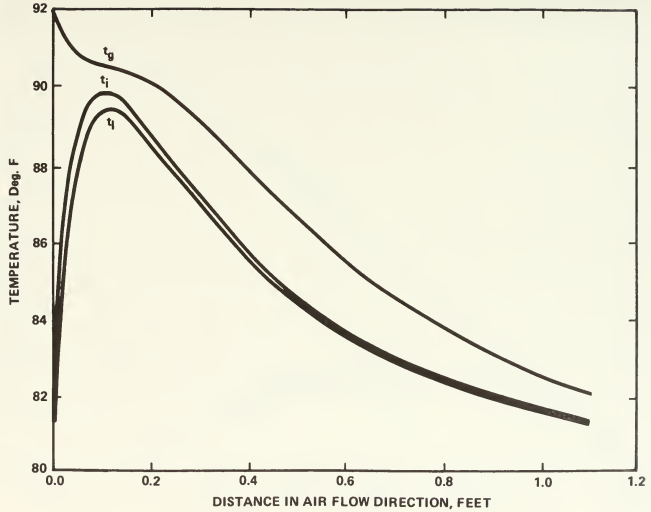

Figure 12. Gas, Interface, and Liquid Temperatures vs. Flow Distance

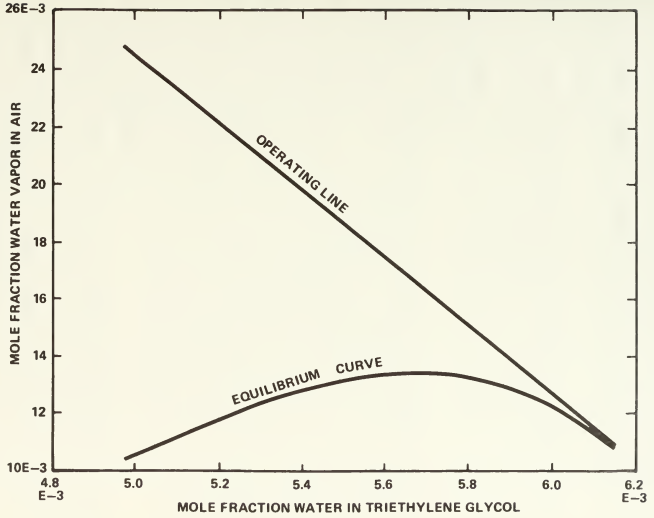

Figure 13. Operating Line and Equilibrium Curve for Dehumidifier Contactor

this reason the 8 and 12 row points may be accepted as exit conditions even though they are not. Figure 14 verifies this point as the 8 row exit marks obtained by iterating the simulation for equal inlet and exit liquid temperatures nearly coincide with the 8 row marks of Figure 10a, the 16 row contactor.

Figure 15 shows the results of an air flow rate which is 75% of the air flow rate of the Figure 14 simulations. Slightly drier, 1.5 grains, and slightly cooler, 1°F, air is the result of a reduced air flow rate on the exit conditions.

Specifying a higher aspect ratio (defined as a greater face area to flow distance ratio for a given volume of contactor) will allow the treatment of more air. Figures 10a and 14 support this statement. For example, the 16 row contactor with a 48" by 127" face area could be arranged as an 8 row contactor with a 96" by 127" face area. This higher aspect ratio contactor will process twice as much air assuming constant TEG recirculation rates and air flow rates per unit face area to exit conditions within 2 to 4 °F and within 2 to 4 grains of the 16 row contactor exit conditions.

An indicative result of an 8 row dehumidifier contactor (from Figures 4 and 10a) is that with 70°F cooling water and 92% inlet TEG concentration the inlet air at 92°F and 111 grains exits at 72.5°F and 56 grains or a dew point temperature of 51°F.

Regenerator Contactor

In assessing the performance of the regenerator contactor the exit TEG concentration is the significant parameter. Figure 16a shows the

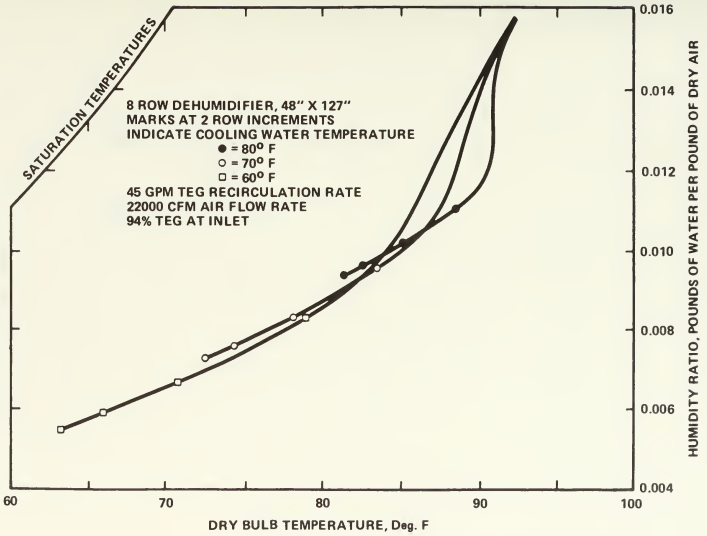

Figure 14. Dehumidifier Operating Lines at 100% Air Flow Rate

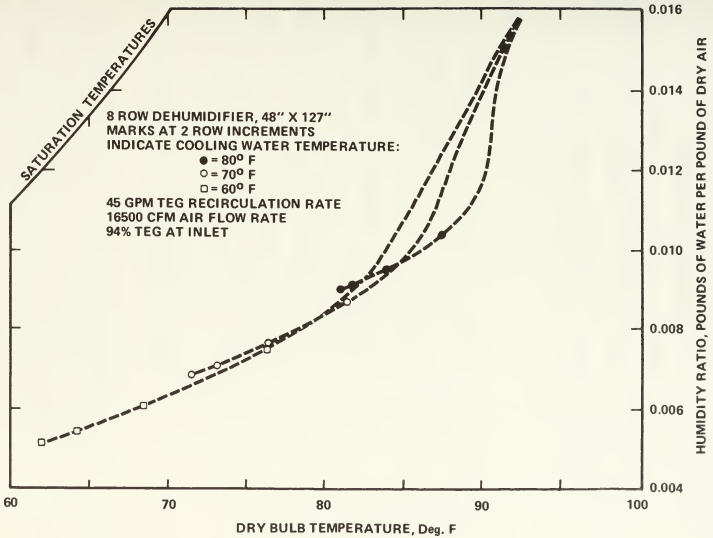

Figure 15. Dehumidifier Operating Lines at 75% Air Flow Rate

ability of the regenerator contactor to concentrate 90% and 92% TEG solution at temperatures of 120°F and 140°F. At constant temperature regeneration the exit concentration variations are less than the inlet concentration variations. For example, at 140°F regeneration, the inlet concentration variation for two simulations is 2% while the exit variation is 1/2%. Figure 16b shows the regenerator operating lines on a psychrometric chart. Both Figures 16a and 16b are for the same simulations.

The regenerator exit conditions are nearly at equilibrium as a study of Figures 16a, 16b and 4 will verify. For example, the nearly 95% exit concentration of Figure 10a for 90% TEG inlet concentration and 120°F heating water corresponds in Figure 10b to 118°F and 0.021 H.R. or 147 grains. On Figure 4 a dry bulb temperature of 118°F and 0.021 H.R. corresponds to an equilibrium humectant value of about 95% (Union Carbide data base). The second equilibrium relationship, equation (2.2), for a contact temperature of 118°F and 95% TEG concentration predicts a vapor pressure of 24.6 mm Hg which corresponds to 0.0208 H.R.

$$Y = 0.622\left(\frac{p}{760 - p}\right) = 0.622\left(\frac{24.6}{735.4}\right) = 0.208 \qquad (6.1)$$

The significant result of the 8 row regenerator contactor simulation is that TEG concentrations of 97% to 97.5% can be achieved with 140°F heating water, and 95% to 96% TEG concentrations can be achieved with 120°F heating water.

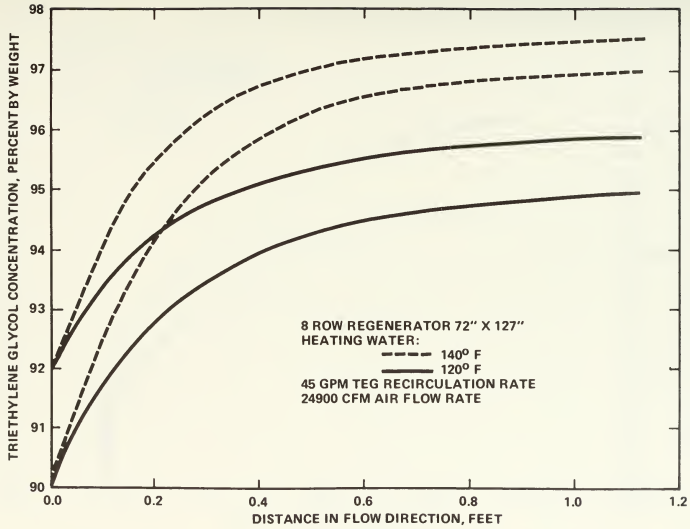

Figure 16a. Regenerator TEG Concentration vs. Flow Distance for Two TEG Inlet Concentrations and Two Heating Water Temperatures

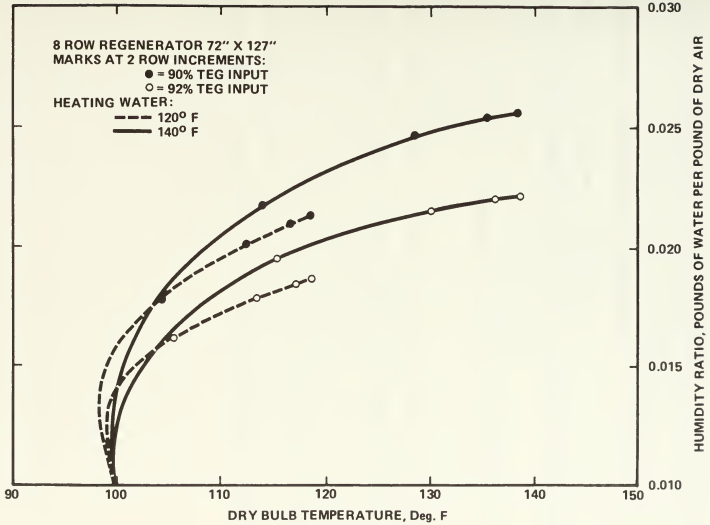

Figure 16b. Regenerator Operating Lines on Psychrometric Chart

VI. CONCLUSIONS

1. Contactor equipment costs may be substantially reduced because half-sized contactors can provide 95% of the dehumidification and 90% of the regenerated TEG concentration as compared to the full sized contactors recommended by the equipment manufacturers.

2. Most effective dehumidification per unit contactor volume occurs at the highest ratio of face area to flow distance.

3. The sensitivity of the regeneration process to the regeneration temperature is minimal.

4. Performance estimates of dehumidification processes which continue to equilibrium can be prepared from Figure 4, Triethylene Glycol Equilibrium Humectant Values on a Psychrometric Chart. First, assume that the exit conditions lie on a vertical line at the cooling water temperature. Then, since each point on the line represents a humidity ratio and a humectant value, and the sum of the air and liquid masses is constant, the equilibrium point can be found.

REFERENCES

1. ASRAE Equipment Handbook, American Society of Heating, Refrigeration and Air Conditioning Engineers, Inc., New York, 1975.

2. ASRAE Handbook of Fundamentals, American Society of Heating, Refrigerating and Air Conditioning Engineers, Inc., New York, 1972.

3. Auslander, D.M., Oster, G.F., Perelson, A. and Clifford, G., "On Systems with Coupled Chemical Reaction and Diffusion," Journal of Dynamic Systems, Measurement and Control, ASME pp. 239-248, September 1972.

4. Baumeister, T., Mark's Standard Handbook for Mechanical Engineers, 7th Ed., McGraw Hill Book Co., New York, 1967.

5. Bird R., Stewart, W., and Lightfoot, E., Transport Phenomena, John Wiley and Sons, Inc., New York, 1960.

6. Carnahan, B. and Wilkes, J., Digital Computing and Numerical Methods, John Wiley and Sons, Inc., New York, 1973.

7. Clark, W., Energy for Survival, The Alternative to Extinction, Anchor Books, Garden City, New York, 1975.

8. Considine, D., Process Instruments and Controls Handbook, 2nd Ed., McGraw Hill Book Co., New York, 1974.

9. Daniels, F., Direct Use of the Sun's Energy, Ballantine Books, New York, 1964.

10. D'Arcangelo, A., Ship Design and Construction, SNA&ME, New york, 1969.

11. Duffie, J. and Beakman, W., Solar Energy Thermal Processes, John Wiley and Sons, Inc., New York, 1974.

12. Gallant, R., Physical Properties of the Hydrocarbons, Vol. 1, Gulf Publishing Co., Houston, Texas, 1968.

13. Karnopp, D. and Rosenberg, R., Analysis and Simulation of Multiport Systems, The Bond Graph Approach to Phyical System Dynamics, The M.I.T. Press, Cambridge, Mass., 1968.

14. Karnopp, D., Rosenberg, R., System Dynamics: A Unified Approach, John Wiley & Sons, Inc., New York, 1975.

15. Kays, W. and London, A., Compact Heat Exchangers, 2nd Ed., McGraw Hill Book Co., New York, 1964.

16. Kays, W., Convective Heat and Mass Transfer, McGraw Hill Book Co., New York, 1966.

17. Kern, D., Process Heat Transfer, McGraw Hill Book Co., New York, 1950.

18. King, J., Separation Processes, McGraw Hill Book Co., New York, 1971.

19. Kothandaraman, C., and Subramanyan, S., Heat and Mass Transfer Data Book, 2nd Ed., John Wiley & Sons, Inc., New York, 1975.

20. Lapedes, D., McGraw-Hill Dictionary of Scientific and Technical Terms, McGraw Hill Book Co., New York, 1976.

21. Lapades, D., McGraw Hill Encyclopedia of Energy, McGraw Hill Book Co., New York, 1976.

22. Löf, G., in Solar Energy Research, ed. F. Daniels and J. A. Duffie, University of Wisconsin Press, 1955.

23. McCabe, W. and Smith, J., Unit Operations of Chemical Engineering, 2nd Ed., McGraw Hill Book Co., New York, 1967.

24. Oster, G. and Auslander, D; "Topological Representations of Thermodynamic Systems-II. Some Elemental Subunits for Irreversible Thermodynamics," Journal of the Franklin Institute, Vol. 292, No. 2, pp. 77-92.

25. Paynter, H., Analysis and Design of Engineering Systems, The M.I.T. Press, Cambridge, Mass., 1961.

26. Perry, R., and Chilton, C., Chemical Engineers Handbook, 5th Ed., McGraw Hill Book Co., New York, 1973.

27. Peters, M. and Timmerhaus, K., Plant Design and Economics for Chemical Engineers, 2nd Ed., McGraw Hill Book Co., New York, 1968

28. Properties and Uses of Glycols, The Dow Chemical Company, 1974.

29. Rohsenow, W. and Choi, H., Heat, Mass and Momentum Transfer, Prentice-Hall Inc., Englewood Cliffs, N.J., 1961.

30. Rohsenow, W. and Hartnett, J., Handbook of Heat Transfer, McGraw Hill Book Co., New York, 1973.

31. Schultz, D. and Melsa, J., State Functions and Linear Control Systems, McGraw Hill Book Co., New York, 1967.

32. Sherwood, T., Pigford, R. and Wilke, C., Mass Transfer, McGraw Hill Book Co., New York, 1975.

33. Staniar, W., Plant Engineering Handbook, 2nd Ed., McGraw Hill Book Co., New York, 1959.

34. Thoma, J., "Bond Graphs for Thermal Energy Transport and Entropy Flow," Journal of the Franklin Institute, Vol. 292, No. 2, pp. 109-120, August, 1971.

35. Thoma, J., Introduction to Bond Graphs and Their Applications, Pargamon Press, New York, 1975.

36. Treybal, R., Mass Transfer Operations, 2nd Ed., McGraw Hill Book Co., New York, 1968.

37. Triethylene Glycol-Water, various graphs, Union Carbide Corp., Research and Development Dept., Tarrytown, N.Y., No. 4-11A3, 1958-59.

APPENDIX A

CONTROL VOLUME DERIVATION OF RATE RELATIONSHIPS

The equations derived in this appendix are concerned with the interphase transfer of mass (water vapor) and energy which occurs during dehumidification of the humid air by the concentrated liquid desiccant. Knowledge of the equilibrium characteristics of the system is necessary for an understanding of the mass transfer operation and, because of simultaneous heat transfer, enthalpy characteristics must also be considered.

Operations such as liquid desiccant dehumidification quickly become complex owing to the mass transfer in both the gas and liquid phases and the large heat effects which accompany condensation and dilution. Furthermore, the need to remove the heat of condensation results in a nonadiabatic operation.

Figure 17 represents the direct contact of the gas (dry air and water vapor) and liquid (TEG and water) flowing side by side in parallel flow and separated by the gas-liquid interface. The changes in temperature, concentration, etc., are all differential over the section.

Based on Figure 17, the balance of this appendix develops:

(1) An overall material balance for control volume III;

(2) Energy balances for control volumes I, II and III;

(3) An interface control volume energy balance.

Next, parameters are separated into catagories and finally, a solution sequence is presented.

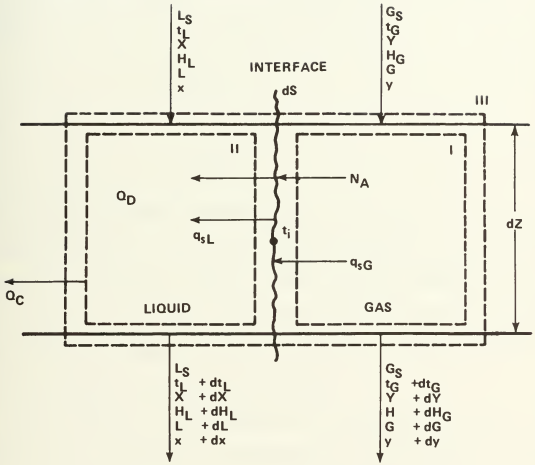

Figure 17. Differential Section of Contactor

The interfacial surface area in the section is dS. For the finned tube contactor the heat transfer area per unit volume, a_H, is known from calculations. Because of the low surface tension of the TEG solution complete wetting of the heat transfer area may be assumed so that the mass transfer area per unit volume, a_M, is equal to the heat transfer area:

$$a_H = a_M \tag{A.1}$$

and,

$$dS = a_M dZ \tag{A.2}$$

where the volume per unit section is dZ.

Consider the mass transfer operation of Figure 17 as conducted in a steady state cocurrent fashion in which L_S and G_S represent the superficial mass flow rate of the non-diffusing pure TEG and dry air respectively. Since the values L_S and G_S are constant through the dehumidifier, they are the basis for the material balance.

At the entrance to the dehumidifier the gas phase contains G total lb/(hr)(sq ft) consisting of non-diffusing G_S lb/(hr)(sq ft) and the diffusing water vapor. The water vapor concentration is given by Y the mass ratio, or equivalently y the mass fraction. The relationships among these variables are:

$$G_S = G(1-y) = \frac{G}{1 + Y} \tag{A.3}$$

$$Y = \frac{y}{1 - y} \tag{A.4}$$

$$y = \frac{Y}{1 + Y} \tag{A.5}$$

Similarly, the liquid consists of L total lb/(hr)(sq ft) containing x mass fraction of water (or mass ratio X) and L_S lb/(hr)(sq ft) of non-diffusing TEG. The relationships among these variables are:

$$L_S = L(1-x) = \frac{L}{1 + X} \tag{A.6}$$

$$X = \frac{x}{1 - x} \tag{A.7}$$

$$x = \frac{X}{1 + X} \tag{A.8}$$

Control Volume III Material Balance

The quantity of water vapor in the gas is Gy lb/(hr)(sq ft). In the liquid it is Lx lb/(hr)(sq ft). Hence the overall material balance about control volume III of Figure 17 for the water is:

$$\underline{\text{In}} = \underline{\text{Out}}$$

$$Lx + Gy = (L+dL)(x+dx) + (G+dG)(y+dy) \tag{A.9}$$

expanding,

$$Lx + Gy = Lx + Ldx + dLx + dLdx + Gy + Gdy + dGy + dGdy \tag{A.10}$$

neglecting the second order terms

$$d(Lx) = -d(Gy) \tag{A.11}$$

or

$$L_S dX = -G_S dY \tag{A.12}$$

The mass transfer rate in lb vapor/(hr)(sq ft) of dehumidifier cross section) is [36]

$$N_A a_M d_Z = -G_S dY \tag{A.13}$$

where

$$N_A = \frac{\text{lb water vapor absorbed}}{(\text{hr})(\text{interfacial surface})} = F_G \ln\left(\frac{1-y^*}{1-y_m}\right) \tag{A.14}$$

Here y* is the equilibrium mole fraction concentration of water vapor over the TEG solution at the interface; y_m is the bulk mole fraction concentration of water vapor in the gas and F_G is the mass transfer coefficient for large mass transfer rates and is defined by Eq. (C.1). Equation (A.14) is a special case for the absorption of one component.

The gas sensible heat transfer rate across the interface in BTU/(hr)(sq ft) is [36]

$$q_{sG} a_H dZ = \frac{N_A C_A}{1-\exp(-N_A C_A/h_G)} (t_G - t_i)\, a_H dZ \tag{A.15}$$

or

$$q_{sG} a_H dZ = h'_G (t_G - t_i) a_H dZ \tag{A.16}$$

where C_A = heat capacity of water vapor at constant pressure, BTU/(lb mass)

h_G = convection heat transfer coefficient, BTU/(hr)(°F)(sq ft interface) and is defined by Eq. (C.2).

Here h'_G includes the effect of mass transfer on heat transfer by accounting for the sensible heat carried by the diffusing water vapor. Radiation has been neglected.

The sensible heat transfer through the liquid in BTU/(hr)(sq ft) is [36]

$$q_{sL}a_H dZ = h_L a_H (t_i - t_L)dZ \tag{A.17}$$

Energy balances around each of the three envelopes of Figure 17 can now be developed.

Envelope I Energy Balance

In = Out

$$G_S H_G = G_S(H_G + dH_G) + q_{sG}a_H dZ + N_A a_M dZ(C_A(t_G - t_o)+\lambda_o) \tag{A.18}$$

where the last term is the enthalpy of the transferred vapor relative to a reference state at t_o where λ_o is the latent heat of vaporization at t_o. Since

$$N_A a_M dZ = -d(Gy) = -d\left(\frac{G_S y}{1-y}\right) = -G_S dY \tag{A.19}$$

substitution yields

$$0 = G_S dH_G + h_G a_H (t_G - t_i)dZ - G_S(C_A(t_G - t_o)+\lambda_o)dY \tag{A.20}$$

The enthalpy of the air-water vapor mixture per pound of dry air is

$$H_G = C_B(t_G - t_o) + Y(C_A(t_G - t_o)+\lambda_o) \tag{A.21}$$

where C_B = heat capacity of dry air at constant pressure,

BTU/(lb)(°F)

Define

$$C_S = C_B + YC_A \tag{A.22}$$

= humid heat of vapor-air mixture, BTU/(lb dry air)(°F)

so that

$$H_G = C_S(t_G - t_o) + Y\lambda_o \tag{A.23}$$

Differentiating equation (A.21)

$$dH_G = C_B dt_G + YC_A dt_G + (C_A(t_G - t_o) + \lambda_o)dY \tag{A.24}$$

or,

$$dH_G = C_S dt_G + (C_A(t_G - t_o) + \lambda_o)\, dY \tag{A.25}$$

Combining with (A.20) gives the envelope I energy balance

$$-G_S C_S dt_G = h_G a_H (t_G - t_i)\, dZ \tag{A.26}$$

Envelope II Energy Balance

In + heat generation = Out

$$L_S H_L + Q_D + N_A a_M dZ C_{AL} (t_i - t_o) + q_{sL} a_H dZ = L_S(H_L + dH_L) + Q_C \tag{A.27}$$

Here

$$Q_C = Ua_C(t_L - t_f)dZ \tag{A.28}$$

= heat removed by cooling coil, BTU/hr

where U = over-all heat transfer coefficient between the liquid and cooling water, BTU/(hr)(sq ft)(°F)

a_C = cooling heat transfer area per unit volume sq ft/cu ft

t_f = cooling water temperature, °F

Substituting equations (A.17) and (A.19) into (A.27) yields

$$Q_D - G_S C_{AL}(t_i - t_o)dY + h_L a_H (t_i - t_L)dZ = L_S dH_L + Q_C \quad (A.29)$$

Here

$$Q_D = N_A a_M dZ H_D = -G_S H_D dY \quad (A.30)$$

= the exothermic heat of dilution (mixing), BTU/hr

where H_D = heat of dilution, BTU/(1b water transferred)

Substituting equations (A.28) and (A.30) into (A.29) yields

$$-G_S(H_D + C_{AL}(t_i - t_o))dY + h_L a_H (t_i - t_L)dZ = L_S dH_L + Ua_C(t_L - t_f)dZ \quad (A.31)$$

The enthalpy of the TEG - water solution per pound of TEG is

$$H_L = C_C(t_L - t_o) + XC_{AL}(t_L - t_o) \quad (A.32)$$

where C_C = heat capacity of TEG at constant pressure
BTU/(1b)(°F)

C_{AL} = heat capacity of liquid water at constant pressure
BTU/(1b)(°F)

Define

$$C_{SL} = C_C + XC_{AL} \quad (A.33)$$

= the humid heat of the TEG-water solution,
BTU/(1b TEG)(°F)

Differentiating equation (A.32)

$$dH_L = (C_C + XC_{AL})dt_L + C_{AL}(t_L - t_o)dX \quad (A.34)$$

or, $dH_L = C_{SL}dt_L = C_{AL}\ (t_L-t_o)dX$ (A.35)

Using equation (A.12)

$$dH_L = C_{SL}dt_L - \frac{G_S}{L_S} C_{AL}\ (t_L-t_o)dY \quad (A.36)$$

Combining with (A.31) gives the envelope II energy balance

$$L_SC_{SL}dt_L = (h_La_HdZ-G_SC_{AL}dY)(t_i-t_L)-G_SH_DdY-Ua_C(t_L-t_f)dZ \quad (A.37)$$

Envelope III Energy Balance

The overall enthalpy balance for control volume III is

In	Out

$$L_SH_L + G_SH_G + Q_D = L_S(H_L + dH_L) + G_S(H_G + dH_G) + Q_C \quad (A.38)$$

Rearranging

$$Q_C = Q_D - L_SdH_L - G_SdH_G \quad (A.39)$$

Substituting into equation (A.37)

$$L_SC_{SL}dt_L = -G_S[C_sdt_G + (C_A(t_G-t_o)-C_{AL}(t_L-t_o)+\lambda_o+H_D)dY] -$$

$$Ua_C(t_L-t_f)dZ \quad (A.40)$$

Interface Control Volume Energy Balance

In	Out

$$N_Aa_MdZ(\lambda_o+C_A(t_G-t_o)) + q_{SG}a_HdZ = N_Aa_MdZ(C_{AL}(t_i-t_o)) + q_{SL}a_HdZ \quad (A.41)$$

Rearranging,

$$N_A a_M (C_A (t_G - t_o) - C_{AL} (t_i - t_o) + \lambda_o) = a_H (h_L (t_i - t_L) - h_G (t_G - t_i)) \qquad (A.42)$$

Solving for t_i

$$t_i = \frac{N_A a_M (C_A (t_G - t_o) + C_{AL} t_o + \lambda_o) + a_H (h_L t_L + h_G t_G)}{N_A a_M C_{AL} + a_H (h_L + h_G)} \qquad (A.43)$$

Parameter Classification

1. Known quantities for which inlet values are given

   t_G, Y, H_G, G, y,

   t_L, X, H_L, L, x,

   t_f

2. Constants

   G_S, C_A, C_B, λ_o,

   L_S, C_{AL}, C_C, H_D,

   U, t_o

3. Variables with known functions

   a_H, a_M, a_C, f_G, h_G, h_L, y*, y_m

By starting at the top of the dehumidifier with the known quantities and solving the equations at each incremental step, dZ, the following quantities will vary;

t_G, Y, H_G, G, y, C_S,

t_L, X, H_L, L, x, C_{SL},

t_i, N_A, Q_D, y^*, y_m,

t_f, Q_C,

and will be obtained after each step and at the exit of the dehumidifier.

Solution Sequence

A solution sequence based on the differential section of Figure 17 is:

$$Y = \frac{y}{1-y} \tag{A.44}$$

water mass ratio,

$$X = \frac{x}{1-x} \tag{A.45}$$

humid heat,

$$C_S = C_B + YC_A \tag{A.46}$$

liquid humid heat,

$$C_{SL} = C_C + XC_{AL} \tag{A.47}$$

gas enthalpy,

$$H_G = C_S(t_G - t_o) + Y\lambda_o \tag{A.48}$$

liquid enthalpy,

$$H_L + C_{SL}(t_L - t_o) \tag{A.49}$$

interface temperature, t_i, from Eq. (A.43);

equilibrium vapor pressure above liquid, p*, from Eq. (2.2);

mole fraction concentration in the gas in equilibrium with the bulk liquid from Henry's Law,

$$y^* = \frac{p^*}{p_t} \tag{A.50}$$

mole fraction concentration in gas,

$$y_m = \frac{y}{0.622 + 0.378\ y} \tag{A.51}$$

mass transfer flux,

$$N_A = F_G \ln\left(\frac{1-y^*}{1-y_m}\right) \tag{A.52}$$

convection gas heat transfer coefficient corrected for simultaneous mass transfer

$$h'_G = \frac{N_A C_A}{1-\exp(-N_A C_A/h_G)} \tag{A.53}$$

This completes the supporting equations for the solution sequence. The derivatives for the solution follow:

$$\frac{dt_G}{dZ} = \frac{-h'_G a_H}{G_S C_S}(t_G - t_i) \tag{A.54}$$

$$\frac{dt_L}{dZ} = \frac{1}{L_S C_{SL}}\left(\left(h_L a_H + C_{AL}\left(-G_S \frac{dY}{dZ}\right)\right)(t_i - t_L) + H_D\left(-G_S \frac{dY}{dZ}\right) - Ua_C(t_L - t_f)\right) \tag{A.55}$$

$$\frac{dt_f}{dZ} = \frac{1}{\dot{m}_f C_{AL}} Ua_C(t_L - t_f) \tag{A.56}$$

$$\frac{dY}{dZ} = -\frac{N_A}{G_S} a_M \tag{A.57}$$

$$\frac{dX}{dZ} = \frac{1}{L_S}\left(-G_S \frac{dY}{dz}\right) \tag{A.58}$$

$$\frac{dy}{dZ} = \frac{1}{(1+Y)^2} \frac{dY}{dZ} \tag{A.59}$$

$$\frac{dx}{dZ} = \frac{1}{(1+X)^2} \frac{dX}{dZ} \tag{.60}$$

$$\frac{d(Gy)}{dZ} = G_S \frac{dY}{dZ} \tag{A.61}$$

$$\frac{d(Lx)}{dZ} = -G_S \frac{dY}{dZ} \tag{A.62}$$

$$\frac{dG}{dZ} = \frac{1}{y}\left(\frac{d(Gy)}{dZ} - G\frac{dy}{dZ}\right) = -N_A a_M \tag{A.63}$$

$$\frac{dL}{dZ} = \frac{1}{x}\left(\frac{d(Lx)}{dZ}\right) - L\frac{dx}{dZ}) = N_A a_M \tag{A.64}$$

Before simulation of the contactor with the solution sequence can proceed, (1) input values must be initialized to correspond to the physical system; (2) equations for fluid properties as functions of temperature and concentration are needed; (3) heat and mass transfer coefficients for the physical system must be predicted or measured; (4) a rational selection of the minimum number of variables necessary to specify the state of the model must be made.

Equations (A.54) through (A.64) above are not all independent. Appendix B describes through bond graph techniques the selection of the minimum number of state variables to represent the LDD contactor. The results of Appendix B indicate that differential equationa (A.54), (A.55), (A.56), (A.63), (A.64) above, plus necessary auxiliary equations, will model the contactor.

APPENDIX B

BOND GRAPH CONTACTOR MODEL

Introduction

The bond graph method developed by Professor H.M. Paynter of MIT for systematic derivation of differential equations for the transport of power is described briefly: Bond graphs are a powerful analytical tool as they give a physical presentation of power flows by maintaining the topological structure of the system while allowing separate determination of the sign of positive power flow and distinction between dependent and independent variables. While each engineering discipline has its own calculation methods, bond graphing is compatible with all disciplines and is invaluable for model development at interfaces, i.e. electrical and fluid. Finally, the transformation from a bond graph to equivalent differential equations follows an exact method.

Bond graph theory has been treated rather thoroughly elsewhere [13], [14], [25], [34], [35]. Thus, only those aspects necessary for understanding the present model development will be discussed and only a meager sampling of the analytical potential of bond graph theory is presented.

General Bond Graph Model

A bond graph representation of a control volume around the gas-liquid interface is shown in Figure 18. This bond graph is a distributed resistance-capacitance model of the interface and can be replicated n times to provide a model of any desired accuracy. Dynamic simulation in time and space is possible with this general model.

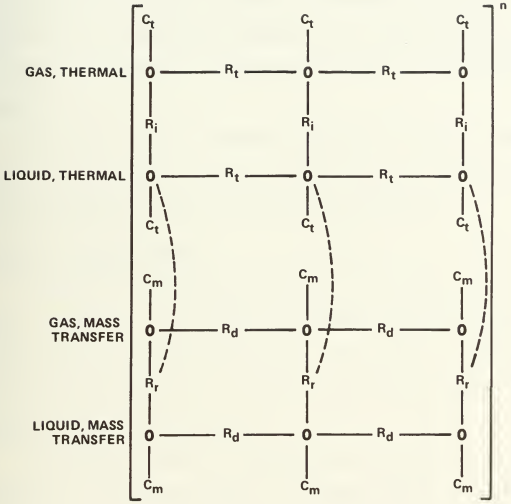

Figure 18. Bond Graph Representation of Coupled Thermal and Mass Transfer Operations in Liquid Desiccant Dehumidification

The zeros represent parallel junctions at which the sum of the heat or mass flows equal zero. A distinct temperature or chemical potential is associated with each zero junction. Two types of capacitances are represented on the graph: thermal, C_t and mass, C_m. There are two types of thermal resistance: convection resistance in the fluids, R_t, and interfacial resistance, R_i. Mass transfer resistance is also of two varieties: diffusion resistance, R_d, and reaction resistance, R_r.

The dotted line is a reaction coupling from the mass transfer portion of the bond graph to the heat transfer portion of the bond graph and represents the heat of condensation and dilution.

Specific Bond Graph Model

Looking at a time invarient solution of the general model allows the n replications to be done with a dynamic simulation routine if the differentials are taken with respect to dZ. Figure 19 shows this specific simplified model with the addition of a cooling medium with heat capacity C_f and temperature t_f.

Bond graphing allows a determination of the number of independent variables by counting the number of storage elements in the model. The temperatures t_g, t_l and t_f are chosen to represent the mass transfer independent variables because of their physical significance and their association with the storage elements. Figure 20 is a word representation of Figure 19 and the contactor. (Note that the t's represent temperature differences.)

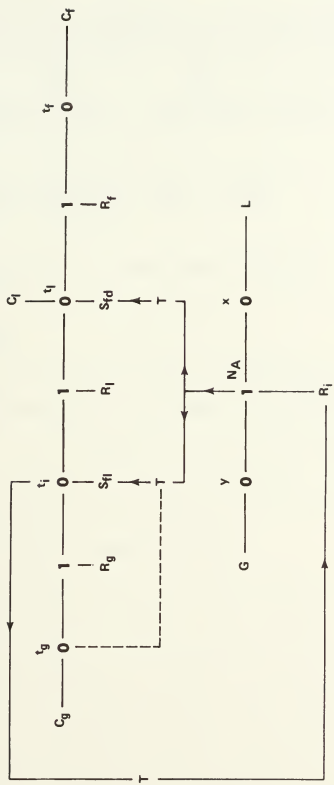

Figure 19. Contactor Bond Graph of Significant Thermal and Mass Transfer Operations

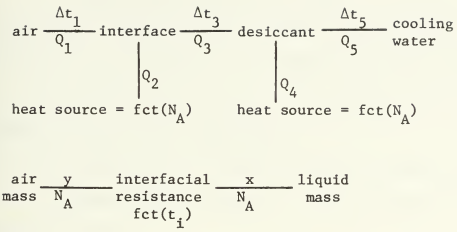

Figure 20. Word Bond Graph of Contactor

Bond Graph Symbols

On Figure 19 the bonds with arrows represent signal flows with no feedback along the same bond. For example, the interfacial resistance to mass transfer, R_i, is dependent on the interface temperature. Solid bonds represent the power flow associated with heat or mass transfer. Ones represent series junctions at which the sum of the efforts, either temperature or chemical potential, is zero.

In a true bond graph the product of the effort variable (above the bond) and the flow variable (below the bond) is power. Figure 19 is a pseudo bond graph because the concentrations are used as the mass transfer efforts rather than chemical potential and because heat flux is used as the thermal flow rather than entropy. With a pseudo bond graph the reaction couplings must be scrutinized as standard bond graph rules do not hold, but with consistent units, pseudo bond graphs follow the remainder of the rules for regular bond graphs. The pseudo bond graph was selected for the physical significance of the effort and flow variables.[14]

A "T" in a signal bond indicates the signal, t_i or N_A, is transformed before use. The dotted line indicates the transformer modulus is controlled by t_g. Linearity is not implied by the bond graph. Two mass flux controlled heat sources, S_{fl} and S_{fd} represent the latent heat of condensation and the heat of dilution.

Heat flux in BTU/(hr)(sq ft) and mass flux in lb water/(hr)(sq ft) are the flow variables used in Figure 19. Table 1 lists the units of the thermal bond graph.

Variable	Units
Effort	°F
Flow	$\frac{\text{BTU}}{(\text{hr})(\text{sq ft})}$
Resistance	$\frac{(\text{hr})(\text{sq ft})(^\circ\text{F})}{\text{BTU}}$
Capacitance	$\frac{\text{BTU}}{(\text{hr})(\text{ft})(^\circ\text{F})}$

Table 1. Thermal Bond Graph Units

Dimensionally, the product of resistance and capacitance is (ft) or the same as the solution increment.

Differential Equation Model

The differential equations which result from a rigorous application of bond graph techniques have been presented as equations (4.1) through (4.5) and are equivalent to equations derived in Appendix A. The computer simulation uses: (1) differential equations (4.1) through (4.5); (2) the auxiliary equation for t_i, Eq. (4.6); (3) the equilibrium relation-

ship for vapor pressure over TEG, Eq. (2.2); and (4) the following sequence of auxiliary equations:

mass fraction in liquid,

$$x = \frac{L - L_S}{L} \tag{B.1}$$

percent weight fraction concentration of TEG,

$$P_T = 100\ (1 - x) \tag{B.2}$$

interface temperature from Eq. (4.6),

$$t_i = fct(t_g, t_l, N_A)$$

equilibrium vapor pressure over TEG from Eq. (2.2),

$$p^* = fct(t_i, P_T)$$

Henry's Law for the mole fraction concentration in the gas in equilibrium with the bulk liquid,

$$y^* = \frac{p^*}{P_t} \tag{B.3}$$

mass fraction in gas,

$$y = \frac{G - G_S}{G} \tag{B.4}$$

mole fraction concentration in gas,

$$y_m = \frac{y}{0.622 + 0.378y} \tag{B.5}$$

mass transfer flux (F_G is derived in Appendix C),

$$N_A = F_G \ln\left(\frac{1 - y^*}{1 - y_m}\right) \tag{B.6}$$

heat of dilution taken as 10% of the heat of condensation and sensible heat associated with the transfered mass,

$$Q_D = N_A \, (100 + (t_i - t_l)) \tag{B.7}$$

mole fraction concentration in liquid,

$$x_m = \frac{x}{8.334 - 7.334\, x} \tag{B.8}$$

and humidity ratio,

$$Y = \frac{y}{1 - y} \tag{B.9}$$

The computer model is now complete.

APPENDIX C

FLUID PROPERTIES AND TRANSFER PARAMETERS

This appendix presents the essential but less than obvious relationships. The development of an equation for the vapor pressure over TEG from graphical data is discussed in Chapter II and is representative of the method of the numerous curve fits presented here. The remaining details may be found in the computer program listing. Appendix E.

Essential to the model is a numerical value for the mass transfer coefficient, F_G. This coefficient is predicted from the more easily obtained gas convection heat transfer coefficient by means of the well accepted Chilton-Colburn analogy. Agreement of the analogy with newer data on mass transfer is very good [32]. The mass and gas heat transfer coefficients are related by

$$F_G = \frac{h_G}{C_B}\left(\frac{Pr}{Sc}\right)^{0.667} \qquad (C.1)$$

where
- F_G = mass transfer coefficient, (lb water)/(hr)(sq ft)
- C_B = heat capacity of air at constant pressure, BTU/(lb mass)
- Pr = Prandtl number
- Sc = Schmidt number
- h_G = heat transfer coefficient between the gas and laminar TEG film, BTU/(hr)(sq ft)(°F)

A numerical value for h_G is based on an empirical correlation for a representative finned tube extended surface heat exchanger reported by Rohsenow [30].

$$h_G = \frac{0.134\, k_B}{D_r}\left(\frac{D_r G_{max}}{\mu_B}\right)^{0.681} (Pr)^{0.333} \left(\frac{s}{l}\right)^{0.2} \left(\frac{s}{t}\right)^{0.113} \qquad (C.2)$$

where

D_r = root diameter of tube, ft

k_B = thermal conductivity of air, BTU/(hr)(ft)(°F)

G_{max} = mass flow rate at minimum cross section, lb/(hr)(sq ft)

s = distance between adjacent fins, in

l = fin height or half the mean fin distance between tubes, in

t = fin thickness, in

μ_B = viscosity of air at bulk temperature, lb/(hr)(ft)

Eq. (C.2) shows excellent agreement with Kays [15] plate finned circular tube data but which geometry differs from the modeled contactor.

A curve fit developed for the Prandtl number for air is

$$Pr = 0.721 \exp(-196E\text{-}6\ t_g) \qquad (C.3)$$

To compute the Schmidt number

$$Sc = \frac{\mu_B}{\rho\, D_v} \qquad (C.4)$$

values for the viscosity, density and diffusivity are needed.

Curve fits led to

$$\mu_B = 0.0223(t_g)^{0.159} \qquad (C.5)$$

and

$$\rho_B = \frac{492\ [18.02\ y + 28.96\ (1-y)]}{359\ \ (460 + t_g)} \qquad (C.6)$$

while the diffusivity is [2]

$$D_v = \frac{0.000146\ (t_g + 460)^{2.5}}{t_g + 901} \qquad (C.7)$$

The thickness of a falling film of the water TEG solution on the vertical aluminum fin is [26]

$$\delta = \left(\frac{3\ \mu_D \Gamma}{\rho_D^2\ g} \right)^{0.333} \qquad (C.8)$$

where δ = film thickness, ft

μ_D = film liquid viscosity, lb/(hr)(ft)

Γ = liquid loading per unit width of fin, lb/(hr)(ft)

ρ_D = density of film liquid, lb/(cu ft)

g = acceleration due to gravity, ft/hr^2

The mass flow rate per unit width Γ can be calculated from the liquid recirculation rate but values for μ_D and ρ_D for TEG-water solutions are obtained from curve fits

$$\mu_D = 4.46\ E\text{-}7(P_T)^{[5.85\ t_1^{(1.487\ -\ 0.727\ \ln\ P_T)}} \qquad (C.9)$$

$$\rho_D = 54.88 + 3.73\ \ln\ P_T - 0.0262\ t_1 \qquad (C.10)$$

The liquid phase heat transfer coefficient was approximated as conduction dominated between the air-liquid interface and the liquid mid-point by

$$h_L = \frac{k_D}{\delta} \qquad (C.11)$$

from the curve fit for the TEG-water solution conductivity

$$k_D = 0.789 - 0.14 \ln P_T - 131E\text{-}6\ t_1 \qquad (C.12)$$

The heat transfer coefficient from the liquid mid-point to the aluminum fin was approximated by the empirical correlation for a falling film [17], [26]

$$h_1 = 55 \left(\frac{k_D\ \rho_D^{1.33} C_D}{L\ \mu_D^{0.333}} \right)^{0.333} \left(\frac{4\ \Gamma}{\mu_D} \right)^{0.111} \qquad (C.13)$$

for

$$\frac{4\ \Gamma}{\mu_D} < 2100$$

where L = length of heat transfer surface, ft

$C_D = C_{SL}$ defined in Eq. (A.33)

A curve fit for the specific heat of the TEG-water solution is

$$C_D = 0.4977 + 0.000444\ t_1 + XC_{AL} \qquad (C.14)$$

A cautionary note with Eq. (C.13), [26] suggested a range of validity on L as 0.4 to 6 ft. Accordingly, the contactor height 1.12 to 2.24 ft was used for L. This gave values for h_1 from 40 to 60 while values for h_L ranged from 150 to 200. These values indicate that Eq. (C.13) may not be used since the heat transfer coefficient can not be less than that of pure conduction. Exclusive use of the conduction coefficient h_L is correct. The best approach is to calculate both h_1 and h_L and use the larger for the entire liquid film. Sole use of h_L produces slightly

cooler operating lines as shown by Figure 21. In addition the typical overall heat transfer coefficient from the liquid to the cooling water increases from 14 to 20 while the typical overall heat transfer coefficient from the air to the cooling water increases from 6 to 7. The comparison in Figure 21 shows that the simulation results are not materially affected.

A curve fit was developed from tube side water heat transfer coefficient data [17]

$$h_t = (0.905 - 0.1863 \ln (\frac{D_r - 2\delta_w}{0.0833}))(163 + 1.731\ t_f)\ V_f^{0.8} \qquad (C.15)$$

where

δ_w = tube wall thickness, ft

V_f = water velocity through tube, ft/sec

The free flow area of Figure 8 is slightly reduced by the TEG-water solution film thickness so that the ratio of free flow area to face area is

$$\sigma = \frac{1 - P(t + 2\delta)(T_{sh} - 12\ D_r)}{T_{sh}} \qquad (C.16)$$

where P = number of fins per inch, 1/in

T_{sh} = horizontal tube spacing, in

The overall heat transfer coefficient from the gas to the cooling water is calculated by

$$U = \frac{1}{\frac{1}{\eta h_G} + \frac{1}{\eta h_L} + \frac{a_H}{a_t}\frac{\delta_w}{k_w} + \frac{a_H}{a_t}\frac{1}{h_t}} \qquad (C.17)$$

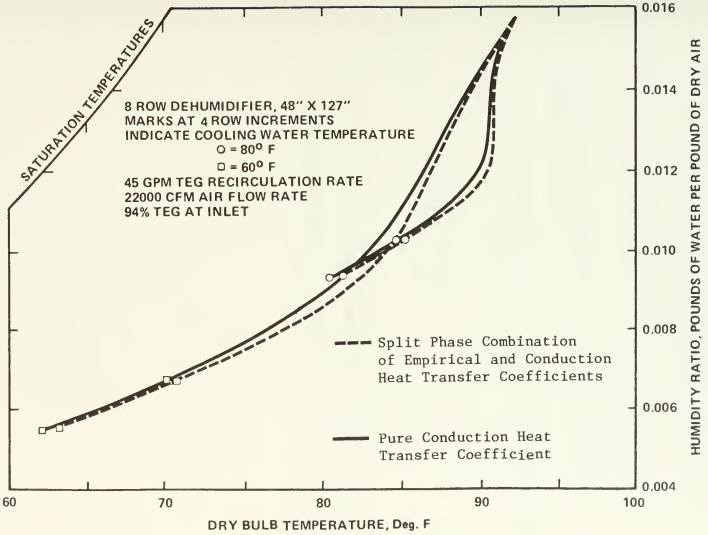

Figure 21. Comparison of Conduction and Combination Liquid Phase Heat Transfer Coefficient

where

a_t = average tube surface area per unit volume, ft^2/ft^3

k_w = conductivity of tube wall, BTU/(hr)(ft)(°F)

δ_w = thickness of tube wall, ft

The calculations were done with the fin efficiency applied to both the fin area and the tube area.

Applying the fin efficiency to the total area instead of just the fin area accounts for 97% of the heat transfer:

$$\frac{\eta}{\eta \frac{a_f}{a_H} + \frac{a_t}{a_H}} = \frac{.66}{.66(.93)+.07} = .97 \qquad \text{(C.18)}$$

The remainder of the contactor geometry and transfer parameter calculations is straight forward. A complete listing may be found in Appendix E.

APPENDIX D

TRIETHYLENE GLYCOL PROPERTIES

Triethylene glycol is a colorless, combustible, hygroscopic water-soluble liquid used as a chemical intermediate, solvent, bactericide, humectant, and fungicide.

Physical Properties [12], [28]:

Formula $CH_2 - O - CH_2 - CH_2 - OH$
$CH_2 - O - CH_2 - CH_2 - OH$

Molecular Weight	150.2
Boiling Point at 1 atm	545.9 °F
Vapor Pressure at 77°F	<0.01 mm Hg
Specific Gravity at 77°F	1.119 g/cc
Freezing point	19 °F
Pour Point	-73 °F
Viscosity at 77°F	37.3 centipoises
Surface Tension at 77°F	45 dynes/cm
Specific Heat at 77°F	0.53 BTU/(lb)(°F)
Flash Point	320 °F
Fire Point	330 °F
Conductivity at 77°F	0.13 BTU/(hr)(ft)(°F)

Desired Desiccant Properties [33]

A liquid desiccant selected for a dehumidification system should have the following characteristics:

1. Suitable vapor pressure characteristics; should be capable of concentration at low temperatures
2. Noncorrosive
3. Odorless
4. Chemical stability; should not break down or vaporize in the range of interest
5. Low viscosity and good heat transfer characteristics; must not crystallize or solidify near the operating range
6. Nontoxic and nonflammable
7. Widely available and inexpensive

Triethylene Glycol Desiccant Properties [12], [28]

1. TEG has a suitable vapor pressure curve and can be concentrated at temperatures as low as 120 °F
2. TEG is compatible with steel if slight TEG discoloration due to iron contamination is acceptable. Otherwise stainless steel, aluminum, or resin coatings should be used.
3. TEG is practically odorless.
4. TEG is a superior choice considering both its hygroscopicity (item 1) and its high boiling point.
5. TEG has a low viscosity and good heat transfer characteristics.
6. TEG is low in chronic oral toxicity. It has been fed in the drinking

water of rats over a two year period at a 4% concentration with no apparent ill effect. Prolonged inhalation of saturated vapors of TEG has produced no ill effects on humans. Flash and fire points determined by the ASTM Cleveland Open Cup method for pure TEG are 320 °F and 330 °F respectively. TEG presents a minimal fire hazard in storage or handling.

7. TEG is a byproduct of automotive antifreeze. The cost of TEG compares to the cost of antifreeze.

APPENDIX E

COMPUTER PROGRAM LISTING

AND

SAMPLE OUTPUT

```
USER=VORTHMA 511 21451    JOINT COMPUTER FACILITY, MIT

      SUBROUTINE EQSIM
      COMMON T,TSTEP,Y(20),F(20),STIME,FTIME,NEWDT,IFWRT,
     *       N,IPR,ICD,ICN,TNEXT,PNEXT,THACK
      IMPLICIT REAL (L)
      REAL NT(3),NTU,NTG
      REAL NG(3)
      DIMENSION YY(3,20),TT(3)
      DIMENSION DBT(7),DPT(7),PT(7),RHM(7),HRM(7),WT(7),LH(7)
      DIMENSION YA(3),YB(3),HL(3)
      DATA DW/62.2/, CAL/1.003/,GRA/4.169E8/,NTG/0./,J/1/,D/0./
      IF (NEWDT) 1,3,2
    1 B=1.
C                    BEGIN INPUT DATA
      CFM=92500.
      DIA=.75
      FP=5.
      FPS=2.
      FT=.01
      GPMLIQ=137.
      LEN=127.
      PTEG=96.
      ROWS=8.
      STEPS=40.
      TF=80.
      TG=92.
      TL=82.
      TUSPH=2.
      TUSPV=1.73
      TUWL=.035
      WAPROX=49.
      WK=8.1
      SH=.01555
      GET CFM,DIA,FP,FPS,FT,GPMLIQ,LEN,PTEG,ROWS,TF,TG,TL,TUSPH,TUSPV,
```

Y(1) = t_f

Y(2) = t_g

Y(3) = t_l

Y(4) = G

Y(5) = L

Y(6) = t_i

Y(7) = y

Y(8) = x

Y(9) = P_T

Y(10) = x_m

Y(11) = N_A

Y(18) = Y

```
USER=VORTHMA 511 21451    JOINT COMPUTER FACILITY, MIT

     *TUWL,WAPROX,SH,STEPS
C                    END INPUT DATA
C                    INITIALIZE DYSYS VARIABLES
      Y(1)=TF
      Y(2)=TG
      Y(3)=TL
      Y(8)=SH/(1.+SH)
      Y(12)=0.
      HOR=.06044*TUSPV
      TCH=HOR
      TSTEP=HOR/STEPS
      FTIME=ROWS*HOR
C          FINNED TUBE HEAT EXCHANGER DIMENSION CALCULATIONS
      ZIN=TUSPV*ROWS*.9653
      Z=ZIN/12.
      TUPR=AINT((WAPROX -TUSPH/2.-1.)/TUSPV+1.5)
      ITPR=IFIX(TUPR)
      GPMPT=FPS*(DIA-TUWL*2.)**2/.4085
      CWFR=GPMPT*TUPR*498.9
      WIDTH=1.+TUSPH/2.+TUSPH*(TUPR-1.)
      CW=CWFR*6./WIDTH
      TUTOT=ROWS*TUPR
      TSA=TUTOT*LEN*.021817*DIA*(1.-FP*FT)
      PFA=.013889*FP*LEN*(WIDTH*Z*12.-TUTOT*.7854*DIA**2)
      TOTSA=PFA+TSA
      FAPTA=PFA/TOTSA
      AH=144.*TOTSA/(WIDTH*LEN*Z)
      AM=AH
      IROW=IFIX(ROWS)
      FTU=LEN*TUTOT/12.
      FR=LEN*WIDTH/144.
C          END EXCHANGER DIMENSION CALCULATIONS                    06
C                    BEGIN FLUID PROPERTIES CALCULATIONS
```

```
USER=VOPTHMA 511 21451    JOINT COMPUTER FACILITY, MIT

      Y(7)=1.-PTEG/100.
      Y(9)=100.*(1.-Y(7))
      VLIQ=4.467E-7*PTEG**5.85*   Y(3)**(1.487-.727*ALOG(PTEG))
      DLIQ=54.88+3.73*ALOG(PTEG)-.0262*Y(3)
      ROF=45.12*GPMLIQ*DLIQ/(FP*LEN*WIDTH)
      REL=4.*ROF/VLIQ
      TEGFT=(3.*VLIQ*ROF/(DLIQ**2*GRA))**.333
      WELL=GRA*DLIQ*TEGFT**2/(10800.*VLIQ)
      SIGMA=(1.-FP*(FT+2.*TEGFT))*(TUSPH-DIA)/TUSPH
      DH=4.*SIGMA/AH
      DGAS=(18.02*Y(8)  +28.96*(1.-Y(8)  ))*492./(359.*(460.+ Y(2)  ))
      GMAX=CFM*60.*DGAS*144./(SIGMA*LEN*WIDTH)
      Y(4)=GMAX*SIGMA/3.
      GS=Y(4)/(1.+Y(8)/(1.-Y(8)))
      FF=Y(4)/(DGAS*3600.)
      GPM=GPMPT*TUPR*ROWS/2.
      AWO=FTU*DIA*37.7/(LEN*WIDTH*Z)
      AWI=FTU*(DIA-TUWL*2.)*37.7/(LEN*WIDTH*Z)
      VGAS=.0223*Y(2)**.159
      REG=GMAX*.0114*.676/(VGAS*DIA)
      STNPRG=EXP(-2.353-.348*ALOG(REG))
      PRG=.721*EXP(-196.E-6*Y(2))
      STG=STNPRG/(PRG**.667)
      GASK=.008*Y(2)**.153
      S=1./FP-FT-12.*TEGFT
      RO=SQRT(TUSPV*TUSPH/3.1416)-DIA/2.
C                 BEGIN TRANSFER PARAMETER CALCULATIONS
      HCG=1.608*GASK*(GMAX*DIA/(VGAS*12.))**.681*PRG**.33*(S/RO)**.2*
     1(S/FT)**.113/DIA
      RG=1./HCG
      DV=1.46E-4*(Y(2)+460.)**2.5/(Y(2)+901.)
      SC=VGAS/(DGAS*DV)
      FG=HCG*(PRG/SC)**.667/.24
```

```
      LIQK=.789-.14*ALOG(PTEG)-131.E-6*Y(3)
      HCL=LIQK/TEGFT
      RL=TEGFT/(2.*LIQK)
      R=(RL+RG)/(RL*RG)
      Y(6)=(Y(2)*RL+Y(3)*RG)/(RG+RL)
      CS=.24+.445*Y(8)/(1.-Y(8))
      CSL=.4977+.000444*TL+CAL*Y(7)/(1.-Y(7))
      LMAX=ROF/TEGFT
      Y(5)=LMAX*FP*TEGFT*7.481
      LS=Y(5)/(1.+Y(7)/(1.-Y(7)))
      GALSUS=TOTSA*TEGFT*7.481
      HFIN=.67*(LIQK**2*DLIQ**1.33*SPA**.67*CSL/(VLIQ**.33*Z))**.33*
     &(4.*LMAX*DH/VLIQ)**.111
      FM=SQRT(2.*HFIN*12./(119.*FT))
      FL=RO/12.
      FEFF=TANH(FM*FL)/(FM*FL)
      HTUBE=(.9095-.1863*ALOG(DIA-2.*TUWL))*(163.+1.731*TF)*FPS**.8
      RW=RL+1./(FEFF*HFIN)+TOTSA*ALOG(DIA/(DIA-2.*TUWL))/(6.283*FTU*WK)
     &+AH/(AWI*HTUBE)
      U=1./(RG+   RW)
      G=Y(4)
      L=Y(5)
      CRG=G*FA*CS/3.
      CRL=L*FA*CSL/3.
      CRGW=GPM*500.*CAL
      NTU=TOTSA*U/(AMIN1(CRG,CRGW)*FA*Z)
      PSYR=HCG/(FG*CS)
      DBT(1)=TG
      HRM(1)=Y(8)/(1.-Y(8))
      PT(1)=PTEG
      PW=29.291*HRM(1)/(HRM(1)+.62198)
      DPT(1)=79.047+30.579*ALOG(PW    )+1.8893*(ALOG(PW    ))**2
      RHM(1)=PW*50.172/(3.195E6*EXP(-7516./(DBT(1)+400.)))
```

```
   90 FORMAT (1H1,53(2H--)/108X,1HI/11X,1HO,41X,1HO,42X,1HO/////////9X,
     15(2H* ),45HFINNED TUBE EXCHANGER SURFACE CHARACTERISTICS, 5(2H *)
     2//9X,8HGAS SIDE,4X,18HHYDRAULIC DIAMETER,9X,F7.4,3H FT,6X,9HFIN PI
     3TCH,13X,F5.2,3X,4HF/IN/ 21X,15HAREA PER VOLUME,10X,F5.1,4X,4H1/FT,
     44X,13HFIN THICKNESS,10X,F5.4,3H IN/ 21X,22HFREE FLOW A PER FACE A,
     55X,F5.3,10X,10HFIN LENGTH,12X,F5.2,3H IN/ 21X,23HFIN AREA PER TO
     6TAL AREA,4X,F5.3,10X,8HFIN AREA,10X,F7.0,5X,5HSQ FT/ 21X,22HFIN MA
     7TERIAL: ALUMINUM,20X,18HTOTAL SURFACE AREA, F7.0,5X,5HSQ FT)
   91 FORMAT (1HO,8X,25HFLUID SIDE TUBE DIAMETER,14X,F5.3,4H IN,6X,
     113HFEET OF TUBES,7X,F5.0,5X,2HFT/ 21X,26HTUBE SPACING HORIZONTAL
     2 ,F5.2,5H IN,6X,11HTUBING AREA,9X,F5.0,5X,5HSQ FT/ 21X,21HTUBE S
     3PACING VERTICAL,5X,F5.2,5H IN,6X,17HAREA O PER VOLUME,4X,F6.2,
     47H 1/FT/21X,13HTUBES PER ROW,12X,I3,14X,17HAREA I PER VOLUME,4X,
     5F6.2,7H 1/FT/ 21X,14HNUMBER OF ROWS,12X,I2,14X,19HTUBE WALL THIC
     6KNESS,4X,F5.3,4H IN// 9X,4HCORE,8X,6HLENGTH,18X,F5.0,5X,2HIN,6X,
     79HFACE AREA,12X,F5.1,4X,5HSQ FT/ 9X,17HDIMENSIONS WIDTH,20X,F5.1,
     84X,2HIN,6X,6HHEIGHT,16X,F4.1,4X,2HIN)
   92 FORMAT (1HO,8X,5(2H* ),16HFLUID PROPERTIES,5(2H *)/ 51X,3HGAS,17X,
     16HLIQUID,9X,13HCOOLING WATER/ 9X,17HINLET TEMPERATURE,5X,1HF,19X,
     2F5.1,2(15X,F5.1)/ 9X,7HDENSITY,15X,8HLB/CU FT,13X,F6.4,13X,F4.1,
     316X,F4.1/7X,15H HEAT CAPACITY,9X,8HBTU/LB F,13X,3(F5.3,15X)/ 9X,
     4 12HCONDUCTIVITY,10X,11HBTU/HR FT F,10X,2(F5.3,15X)/ 9X,9HVISCOS
     5ITY,13X,8HLB/HR FT,13X,F5.3,13X,F5.1/ 9X,14HPRANDTL NUMBER,29X,F5.
     663/ 9X,15HREYNOLDS NUMBER,25X,F5.0,13X,F5.3/ 9X,14HSCHMIDT NUMBER,
     729X,F6.4/ 9X,14HSTANTON NUMBER,29X,F6.4/ 9X, 8HVELOCITY,14X,6HFT/S
     8EC,14X,F5.2,16X,F5.3,14X,F5.2/ 9X,14HMASS FLOW RATE,8X,11HLB/HR SQ
     9 FT,7X,F5.0,15X,F5.0,14X,F7.1/ 9X,13HCAPACITY RATE,9X, 8HBTU/HR F,
     *8X,F7.0,13X,F7.0,12X,F8.0/ 9X,18HFFG FILM THICKNESS,4X,2HFT,35X,
     1F8.5,/ 9X,13HTEG SUSPENDED,9Y,3HGAL,36X,F5.1)
   93 FORMAT (1H1,53(2H--)/108X,1HI/11X,1HO,41X,1HO,42X,1HO/////////9X,
     1 5(2H* ),19HTRANSFER PARAMETERS,5(2H *)//51X,3HGAS,17X,6HLIQUID,9
     2X,13HCOOLING WATER//9X,16HFILM COEFFICIENT, 6X,14HBTU/HR SQ FT F,6
     3X,F5.2,2(14X,F6.1)//9X,33HOVERALL HEAT TRANSFER COEFFICIENT,9X,F5.
```

```
USER=VORTHMA 511 21451    JOINT COMPUTER FACILITY, MIT

     42,3X,14HBUT/HR SQ FT F/9X,33HOVERALL MASS TRANSFER COEFFICIENT,7X
     5F7.2,3X,20HLB MASS H2O/HR SQ FT// 9X,42HNUMBER OF HEAT TRANSFER UN
     6ITS PER VOLUME  ,F6.3,9H  1/CU FT,13X,9H(NTU/VOL)/
     7                          /9X,19HPSYCHROMETRIC RATIO,23X,F6.3/)
    94 FORMAT (1HO,8X,5(2H* ),24HPSYCHROMETRIC PROPERTIES,5(2H *)// 62X,
     15HINPUT,                    19X,6HOUTPUT//
     29X,20HDRY BULB TEMPERATURE,5X,1HF,         26X,F6.1,19X,F6.1/
     39X,21HDEW POINT TEMPERATURE,4X,1HF,         26X,F6.1,18X,F6.1//
     49X,26HTSG WEIGHT CONCENTRATION %,           27X,F6.2,18X,F6.2//
     59X,17HRELATIVE HUMIDITY,8X,1H%,          26X,F6.1,19X,F6.1  / 9X,38H
     6HUMIDITY RATIO    LB H2O/LB DRY AIR    ,      17X,F6.4,18X,F6.4//9X,
     717HWATER TRANSFERRED,5X,9HLB H2O/HR,            45X,F6.1/
     89X,29HLATENT HEAT EVOLVED   KBTU/HR,            45X,F8.1)
    95 FORMAT (1H1)
       PUT HOR,TCH,TSTEP,FTIME,ZIN,Z,TUPR,ITPR,GPMPT,CWFR,WIDTH,CW,
     1TUTOT,TSA,PFA,TOTSA,FAPTA,AH,IROW,FTU,FA,VLIQ,DLIQ,ROF,REL,
     2TEGFT,VELL,SIGMA,DH,DGAS,GMAX,GS,FF,GPM,AWO,AWI,VGAS,REG,
     3STNPRG,PRG,STG,GASK,S,HCG,RG,DV,SC,FG,LIQK,HCL,RL,CS,CSL,LMAX,
     4LS,GALSUS,HFIN,RO,FM,FL,FEFF,HTUBE,RW,U,G,L,CRG,CRL,CRCW,NTU
       J=2

     2 Y(9)=100.*(1.-Y(7))
       LH(J+4)=LH(J+4)+HL(J)*AM*FA*TSTEP/1000.
       YIM=(EXP(-9259./(Y(6)+460.)+20.407-1.433*((1./(.5+100.*Y(7)))**
     &1.5)+3.715*((1.-(100.*(1.-Y(7))/99.5)**3)**.167-1.)))/760.
       Y(10)= Y(8)/(.622+.378*Y(8))
       Y(11)=FG*ALOG((1.-YIM)/(1.-Y(10)))
       Y(13)=(Y(6)-Y(2))/RG
       Y(14)=HD+HL(2)
       CG=GS*(.24+(Y(8)*.445)/(1.-Y(8)))/(24.*FP)
       CL=LS*(.4977+.000444*Y(3)+Y(7)/(1.-Y(7)))/(24.*FP)
    15 Y(15)=YIM
       IF (T .LT. (FTIME-TSTEP)) GO TO 6
```

```
      DBT(J+4)=Y(2)
      HRM(J+4)=Y(8)/(1.-Y(8))
      PT(J+4)=Y(9)
      PW=29.291*HRM(J+4)/(HRM(J+4)+.62198)
      DPT(J+4)=79.047+30.579*ALOG(PW       )+1.8893*ALOG(PW       )**2
      RHM(J+4)=PW*50.172/(3.195E6*EXP(-7516./(DBT(J+4)+400.)))
      ST(J+4)=(G-Y(4))*FA
      B=B+1.
      IF (B .GT. 1.01*ROWS) GO TO 8
      IF (B .GE. 2.) TSTEP=HOR/40.
      PUT 6,0, B,TSTEP,J
    6 Y(16)= Y(7)/(8.334-7.334*Y(7))
      Y(17)=ABS(Y(10)-Y(15))
      Y(18)=Y(8)/(1.-Y(8))
      YI=YIM/(1.608-.608*YIM)
      Y(19)=YI/(1.-YI)
      Y(20)=AMAX1(ABS(Y(11)),.0001)
      HL(J)=Y(11)*(.445*Y(2)+1094.)
      IF (T .GE. (FTIME-TSTEP)) GO TO 8

    3 Y(7)=(Y(5)-LS)/Y(5)
      Y(8)=(Y(4)-GS)/Y(4)
      YIM=(EXP(-9259./(Y(6)+460.)+20.407-1.433*((1./(.5+100.*Y(7)))**
     &1.5)+3.715*((1.-(100.*(1.-Y(7))/99.5)**3)**.167-1.)))/760.
      Y(10)= Y(8)/(.622+.378*Y(8))
      HD=100.*Y(11)
      Y(11)=FG*ALOG((1.-YIM)/(1.-Y(10)))
      F(1)=(Y(3)-Y(1))/(CW*RW)
      F(2)=(Y(6)-Y(2))/(CG*RG)
      F(3)=((Y(1)-Y(3))/RW+(Y(6)-Y(3))/RL+HD)/CL
      F(4)=-Y(11)*AM
      F(5)=Y(11)*AM
      Y(6)=(Y(11)*   (1094.+.445*Y(2))+Y(2)/RG+Y(3)/RL)/(Y(11)   +B)
```

```
       USER=VORTHMA 511 21451    JOINT COMPUTER FACILITY, MIT

             GO TO 9
           8 WRITE (5,90) DH,FP,AH,FT,SIGMA,RO,FAPTA,PFA,TOTSA
             WRITE (5,91) DIA,FTU,TUSPH,TSA,TUSPV,AWO,IIPR,AWI,IROW,TUWL,LEN,
            &             FA,WIDTH,ZIN
             WRITE (5,92) TG,TL,TF,DGAS,DLIQ,DW,CS,CSL,CAL,GASK,LIQK,VGAS,VLIQ,
            &PRG,REG,REL,SC,STG,FF,VELL,FPS,G,L,CWFR,CRG,CRL,CRCW,TEGFT,GALSUS
             WRITE (5,93) HCG,HCL,HTUBE,U,FG,NTU,PSYR
             WRITE (5,94) DBT(1),DBT(6),DPT(1),DPT(6),PT(1),PT(6),RHM(1),RHM(6)
            *,HRM(1),HRM(6),WT(6),LH(6)
             WRITE (5,95)
             PUT Y
             T=FTIME
           9 CONTINUE
             RETURN
             END
PROGRAM  EQSIM  HAS     NO ERRORS
```

* * * * * FINNED TUBE EXCHANGER SURFACE CHARACTERISTICS * * * * *

GAS SIDE	HYDRAULIC DIAMETER	0.0210	FT	FIN PITCH	5.00	F/IN
	AREA PER VOLUME	112.2	1/FT	FIN THICKNESS	0.0100	IN
	FREE FLOW A PER FACE A	0.586		FIN LENGTH	0.67	IN
	FIN AREA PER TOTAL AREA	0.928		FIN AREA	4908.	SQ FT
	FIN MATERIAL: ALUMINUM			TOTAL SURFACE AREA	5287.	SQ FT
FLUID SIDE	TUBE DIAMETER	0.750	IN	FEET OF TUBES	2032.	FT
	TUBE SPACING HORIZONTAL	2.00	IN	TUBING AREA	379.	SQ FT
	TUBE SPACING VERTICAL	1.73	IN	AREA O PER VOLUME	8.47	1/FT
	TUBES PER ROW	24		AREA I PER VOLUME	7.68	1/FT
	NUMBER OF ROWS	8		TUBE WALL THICKNESS	0.035	IN
CORE DIMENSIONS	LENGTH	127.	IN	FACE AREA	42.3	SQ FT
	WIDTH	48.0	IN	HEIGHT	13.4	IN

* * * * * FLUID PROPERTIES * * * * *

		GAS	LIQUID	COOLING WATER
INLET TEMPERATURE	F	92.0	61.8	60.0
DENSITY	LB/CU FT	0.0715	70.1	62.2
HEAT CAPACITY	BTU/LB F	0.247	0.612	1.003
CONDUCTIVITY	BTU/HR FT F	0.016	0.148	
VISCOSITY	LB/HR FT	0.046	92.0	
PRANDTL NUMBER		0.708		
REYNOLDS NUMBER		2737.	0.243	
SCHMIDT NUMBER		0.6083		
STANTON NUMBER		0.0112		
VELOCITY	FT/SEC	9.29	0.024	2.00
MASS FLOW RATE	LB/HR SQ FT	2391.	186.	27106.9
CAPACITY RATE	BTU/HR F	2778.	1610.	108993.
TEG FILM THICKNESS	FT		0.00085	
TEG SUSPENDED	GAL		33.6	

* * * * * TRANSFER PARAMETERS * * * * *

		GAS	LIQUID	COOLING WATER
FILM COEFFICIENT	BTU/HR SQ FT F	11.54	174.3	456.0
OVERALL HEAT TRANSFER COEFFICIENT		6.13	BUT/HR SQ FT F (GAS TO COOLING WATER)	
OVERALL MASS TRANSFER COEFFICIENT,FG		53.19	LB MASS H2O/HR SQ FT	
NUMBER OF HEAT TRANSFER UNITS PER VOLUME		0.248	1/CU FT	(NTU/VOL)
PSYCHROMETRIC RATIO		0.878		

* * * * * PSYCHROMETRIC PROPERTIES * * * * *

		INPUT	OUTPUT
DRY BULB TEMPERATURE	F	92.0	62.7
DEW POINT TEMPERATURE	F	69.4	42.9
T&G WEIGHT CONCENTRATION	%	92.00	88.26
RELATIVE HUMIDITY	%	49.1	49.3
HUMIDITY RATIO	LB H2O/LB DRY AIR	0.0158	0.0059
WATER TRANSFERRED	LB H2O/HR		982.0
LATENT HEAT EVOLVED	KBTU/HR		1147.5

Thesis
V983 Vorthman
An analysis of a liquid desiccant dehumidifier regenerated with waste or solar power.
171193